EARTH SCIENCES
RESEARCH JOURNAL

Earth Sci. Res. J. Vol. 12, No. 1 (June 2008): 72-106

PETROGENESIS OF THE METACARBONATE AND RELATED ROCKS OF THE SILGARÁ FORMATION, CENTRAL SANTANDER MASSIF, COLOMBIAN ANDES: AN OVERVIEW OF A "REACTION CALCIC EXOSCARN"

Ríos, C.A.[1]***, Castellanos, O.M.***[2]***, Gómez S.I.***[2] ***and Ávila, G.A.***[2]

[1] *Escuela de Geología, Universidad Industrial de Santander, Bucaramanga, Colombia*
[2] *Programa de Geología, Universidad de Pamplona, Colombia.*

Abstract

Metacarbonate rocks (pure and impure marbles, carbonate-silicate rocks, calc-silicate rocks and carbonate-bearing silicate rocks) form a very complex group within the metamorphic sequence of the Silgará Formation at the central Santander Massif (CSM). These rocks are interpreted as derived from a sedimentary sequence (including limestones and dolostones, carbonate-bearing mudstones, sandstones, tuffaceous and evaporitic sediments and marlstones) overprinted by near-isochemical regional metamorphism. They usually appear as scarce intercalations from millimeter up to meter scale, within the high-grade pelitic rocks, in the lower part of the metamorphic section, although the proportion of metacarbonate rocks can be higher and different marble layers are exploited. We report for the first time the occurrence of a "reaction calcic exoskarn", which corresponds to such metacarbonate rocks, taking into account that a skarn can be developed during regional metamorphism and by different metasomatic processes, adjacent to intrusive bodies, along faults and shear zones, and what defines these rocks as a skarn is its mineralogy, which includes a variety of calc-silicate and associated minerals, usually dominated by garnet and pyroxene. Therefore, this paper focus attention to the occurrence of metacarbonate and related rocks, which occurs as small scale reactions zones that show a gradational contact from garnet-bearing pelitic rocks to marbles or carbonate-silicate rocks, giving particular interest to the calc-silicate rocks, which are characterized by the presence of elongated grains of banded clinopyroxene (diopside) and scapolite and massive or scattered garnet. Several reaction-zones occur in the contact between impure calcite marble and garnet-bearing metapelite and the sequence of mineral assemblages in these reaction zones is: biotite + plagioclase ± K-feldspar ± garnet (Zone I), biotite + plagioclase ± K-feldspar ± garnet ± staurolite ± epidote (Zone II), plagioclase + amphibole ± garnet ± epidote (Zone III), amphibole + diopside + garnet + plagioclase (Zone IV),

Manuscript received October 13 2007.
Accepted for publication December 20 2007.

plagioclase + diopside ± scapolite (Zone V), epidote ± calcite (Zone VI), and calcite ± dolomite (Zone VII).

Key words: Metacarbonate; Silgará Formation; exoskarn; diopside; garnet

Resumen

Las rocas metacarbonatadas (mármoles puros o impuros, rocas carbonatosilicatadas, rocas calcosilicatadas y rocas silicatadas con presencia de carbonato) forman un grupo muy complejo dentro de la secuencia metamórfica de la Formación Silgará en la región central del Macizo de Santander. Estas rocas son interpretadas como derivadas de una secuencia sedimentaria (incluyendo calizas y dolomías, lodositas con presencia de carbonato, areniscas, sedimentos tobáceos y evaporíticos y margas) afectada por metamorfismo regional casi isoquímico. Ellas usualmente ocurren como esazas intercalaciones a escala milimétrica a métrica, dentro de las rocas pelíticas de alto grado, en la parte inferior de la sección metamórfica, aunque la proporción de rocas metacarbonatadas puede se mas alta y diferentes niveles de mármol son explotados en esta región. Aquí reportamos por primera vez la ocurrencia de un "exoskarn cálcico de reacción", el cual corresponde a tales rocas metacarbonatadas, tomando en cuenta que un skarn puede desarrollarse como consecuencia del metamorfismo regional y por diferentes procesos metasomáticos, adyacente a cuerpos intrusivos, a lo largo de fallas y zonas de cizallamiento, y lo que define estas rocas como un skarn es su mineralogía, la cual incluye una variedad de minerales calcosilicatados y asociados, usualmente dominados por granate y piroxeno. Por lo tanto, este articulo esta enfocado a la presencia de rocas metacarbonatadas y asociadas, las cuales ocurren como zonas de reacción a pequeña escala que muestran un contacto gradacional desde rocas pelíticas con presencia de granate hasta mármoles o rocas carbonatosilicatadas, dando particular interés a las rocas calcosilicatadas, las cuales se caracterizan por la presencia de cristales alargados de clinopiroxeno (diópsido) y escapolita bandeados y granate masivo o disperso. Varias zonas de reacción ocurren en la interfase entre mármol y metapelita con granate y la secuencia de paragenesis minerales en estas zonas de reacción is: biotita + plagioclasa ± feldespato potasico ± granate (Zona I), biotita + plagioclasa ± feldespato potasico ± granate ± estaurolita ± epidota (Zona II), plagioclasa + anfíbol ± granate ± epidota (Zona III), anfíbol + diopsido + granate + plagioclasa (Zona IV), plagioclasa + diopsido ± escapolita (Zona V), epidota ± calcita (Zona VI), y calcita ± dolomita (Zona VII).

Palabras claves: Metacarbonatadas; Formación Silgará; exoskarn; diópsido; granate

Introduction

The Santander Massif is situated in the Eastern Cordillera of the Colombian Andes, where the cordillera is divided into the NE-SW-trending Perijá Range and the ENE-WSW-trending Mérida Andes of Venezuela (FIGURE 1), and constitutes a natural laboratory for the learning and understanding of geologic processes that have occurred in northern Andes Codillera and is one of the most investigated regions in Colombia. Different studies (Restrepo-Pace, 1995; Restrepo-Pace *et al.*, 1997; Schäfer *et al.* 1998; García y Ríos, 1998, 1999; Campos, 1999; García y Castellanos, 1998; García y Ríos, 1999; Montenegro y Barragán, 1999; Ríos, 1999, 2001; Ríos and Takasu, 1999, 2000; Ríos and García, 2001a, 2001b; García y Campos, 2000; Castellanos, 2001; Mantilla *et al.*, 2001; 2002; 2003; Gélvez and Márquez, 2002; Ríos *et al.* 2003a, 2003b; Cardona, 2003; Castellanos *et al.*, 2004; García et al, 2005; Ríos, 2005; Gómez y Avila, 2006) have been carried out during the last 20 years in this region and most of these were directed toward an estimate of the conditions of metamorphism. Its pre-Devonian metamorphic complex has been classically divided into three geologic units in ascending order of tectono-stratigraphic level:

Bucaramanga Gneiss Complex, Silgará Formation and Orthogneiss, which are cut by Mesozoic and Tertiary igneous bodies (Goldsmith *et al.*, 1971; Banks *et al.*, 1985; Boinet *et al.*, 1985; Dörr *et al.*, 1995; Restrepo-Pace, 1995; Ordoñez, 2003; Ordóñez and Mantilla, 2005). Sedimentary rocks ranging in age from Devonian to Tertiary flank the core rocks (Ward *et al.*, 1973). At the central Santander Massif (CSM), Ríos and co-workers have carried out studies on the geologic evolution of the different metamorphic units that crop out in this region, making emphasis on the Silgará Formation metamorphic rocks, in which they have defined a metamorphic zonation, modifying the metamorphic isograds reported by Ward *et al.* (1970), revealing a complex metamorphic and deformational history for this geologic unit. The Silgará Formation at the CSM is mainly composed by pelitic rocks with lesser amounts of psammitic, semipelitic, metabasic, as well as metacarbonate rocks, which were affected by a Caledonian regional metamorphism, developing a metamorphic zonation from the biotite zone through garnet and staurolite-kyanite zones up to the sillimanite zone of the typical Barrovian zonal scheme at medium pressure conditions. The rocks of interest in this paper are referred to as the metacarbonate and related rocks, which can be interpreted as reaction zones of diffusion metasomatic origin, formed by interactions between original thin limestone layers and adjacent pelitic rocks, such as those described by Brady (1977) and Joesten (1977; 1991), which are characterized by the development of narrow, multi-layered, reaction zones with different high-variance mineral assemblages. Campos (1999) performed a first attempt to characterize the main mineralogical, textural and structural changes occurring in metasomatic zones developed between garnet-bearing metapelite and marble of the Silgará Formation at the CSM, which were recently studied in detail by Gómez y Avila (2006), defining different reaction bands. In this paper, we carried out a petrological study of these zones of metasomatic reaction to determine their probable protolith and origin, which is also important to evaluate the P-T-fluid evolution of a metamorphic complex sequence such as the Silgará Formation, although the role of fluids during regional metamorphism is often obscure due to the complexity of the rocks. Therefore, this work differs somewhat from previous studies, because it deals with a great variety of metacarbonate and related rocks but little variation in metamorphic grade. Another aim of the study was to discern the metasomatic effect associated to the emplacement of a nearby orthogneiss mass as previously has been reported by Campos (1999). The characterization of the principal stages of their metamorphic evolution in terms of changes in the intensive variables pressure (P), temperature (T), and composition of the fluid (XCO_2) are based on (1) detailed petrographic study of selected samples, (2) characterization of mineral chemistry by microprobe analyses, and (3) phase relationships.

Geological setting

As illustrated in Figure 1, the crystalline basement at the CSM is composed by the deformed and metamorphosed rocks of the Bucaramanga Gneiss Complex, Silgará Formation and Orthogneiss and the igneous succession developed in two cycles: (1) syn-orogenic magmatism with alkaline affinity during the Paleozoic and (2) post-orogenic magmatism with calc-alkaline affinity during Triassic-Jurassic (Goldsmith *et al.*, 1971; Banks *et al.*, 1985; Boinet *et al.*, 1985; Dörr *et al.*, 1995; Restrepo-Pace, 1995; Ordoñez, 2003; Ordóñez and Mantilla, 2005). The rocks of interest in this study are referred as the Lower Paleozoic Silgará Formation metamorphic sequence that crops out into two N-S trending strips, locally interrupted by the presence of dykes and sills of orthoamphibolites with banded to gabbroic structures. The Silgará Formation is mainly composed by metapelitic rocks with minor intercalated psammitic, semipelitic, metabasic and metacarbonate rocks (Figure 3), which were affected by a Caledonian regional metamorphism produced a metamorphic zonation from the biotite zone through the garnet and staurolite-kyanite zones up to the sillimanite zone of the typical Barrovian zonal scheme under low- to high-temperature and medium-pressure conditions.

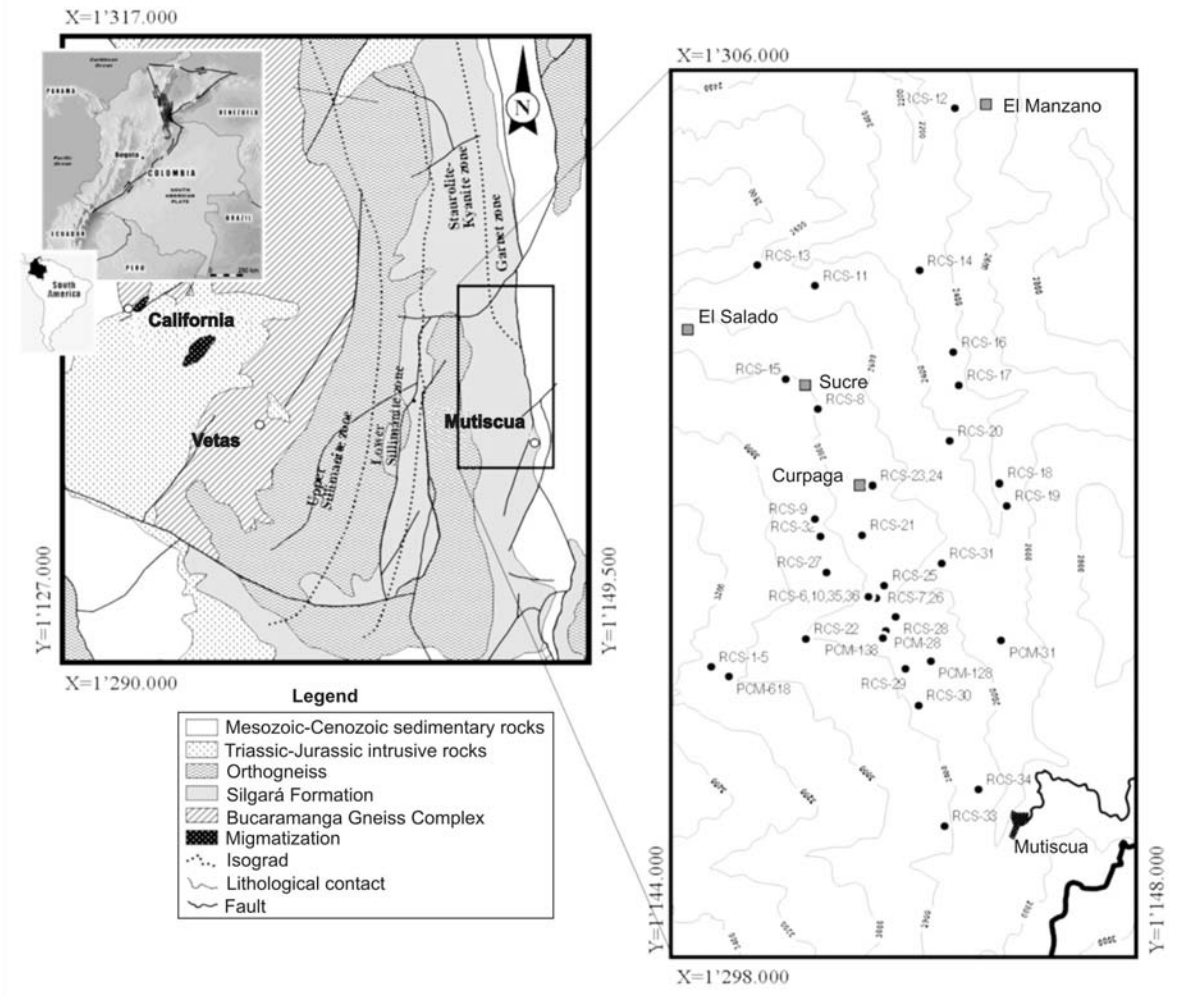

Figure 1. Generalized geological map of the central Santander Massif modified from Ward *et al*. (1970) and Garcia *et al*. (2005), showing the study area as well as the sampling localities of metacarbonate and related rocks (adapted and modified from Gómez y Ávila, 2006).

Gómez y Ávila (2006) carried out a study of the metamorphic sequence cropping out along the Valegra stream, making emphasize on the metacarbonate and associated rocks that occur in the contact between marble and polite layers. A broad spectrum of physical conditions, varying from greenschist facies to amphibolite facies, have been attributed to the investigated metamorphic sequence. Recent studies (García y Ríos, 1999; Campos, 1999; Montenegro y Barragán, 1999; García y Campos, 2000; Castellanos, 2001; Castellanos *et al.*, 2004; García *et al.*, 2005) reveal a complex metamorphic and deformational history of this geological unit. Castellanos (2001) report for the first time P-T conditions of metamorphism based on a petrological study of the Silgará Formation metapelitic rocks at the CSM. García *et al.* (2005) present additional evidence on the metamorphic conditions of these rocks, suggesting a P-T path. However, respect to the tectono-metamorphic evolution of the Silgará Formation, there are still scarce studies that have been done so far. Metapelitic rocks were the focus of this study because they are highly sensitive to changes in pressure and temperature conditions and preserve

textural, structural and mineralogical evidence that provide important clues to constrain the tectono-metamorphic evolution of Silgará Formation at the CSM. The Silgará Formation pelites show overprinting relationships allowing the recognition of three main deformation events (D_1, D_2, and D_3) at the CSM, and during the last stage it has been affected by an extensive retrograde metamorphism.

Field relationships

We adopted the proposal of Rosen *et al.* (2005), which is a basis for a systematic scheme of metacarbonate rock nomenclature proposed by the Subcomission on the Systematics of Metamorphic Rocks, a branch of the Commission on Systematics in Petrology of the International Union of Geological Sciences (IUGS). Metacarbonate rocks occur as scarce intercalations of variable morphology (with sharp contacts) and thickness, developing discontinuous bands and lenticular bodies, within the metamorphic sequence of the Silgará Formation at the central Santander Massif (Figure 2). Marbles show a transition into carbonate-silicate rocks, which, in turn, pass into calc-silicate and carbonate-bearing silicate rocks. Finally, when carbonate tends to disappear in calc-silicate and carbonate-bearing silicate rocks, they pass into metapelitic and metamafic rocks. Calc-silicate rocks show a very complex mineralogy and appear most commonly as green reaction zones along the contact between marbles or carbonate-silicate rocks and pelitic layers of millimeter to centimeter scale, and their regional proportion is difficult to assess due to exposure limitations. Marbles occur as white, gray, orange or pale green layers that alternate with pelitic and calc-silicate rocks, and their thickness ranges from several centimeters up to meter scale. The fabric of these rocks is characterized by weak to strong banding that defines the foliation of the rocks, and is commonly affected by isoclinal folds. The banding is characterized by the alternation of carbonate-rich zones (from millimeter to centimeter scale) with pelitic and/or calc-silicate layers. The reaction zones are parallel to the main foliation and in many cases have been folded with it. Gradational contacts between garnet-bearing pelitic schists to marbles or carbonate-silicate rocks were also observed, and are especially abundant in strongly deformed rocks, where calc-silicate zones may have a very irregular shape and variable thickness (up to several centimeters). Other rocks associated to the investigated metacarbonate sequence correspond to the Devonian Floresta Formation, which were not considered in this study, and include calc-schists produced by metamorphism of argillaceous limestones mainly composed by calcite, calc-micaschists composed of calcite, mica and quartz, and low metamorphosed limestones, the last of them occurring along a breccia zone. General macroscopic characteristics of the reaction zones observed between metacarbonate rocks and pelitic schists of the Silgará Formation are shown in Figure 3. On the other hand, Figure 4 depicts schematically the distribution of the reactant lithologies across the studied traverse of samples RCS-1 to RCS-5, and Figure 5 shows the reaction zones determined in sample RCS-29.

Textural relationships and mineral assemblages across the reaction zones

A petrographic study, including mineral assemblages and reaction textures, was carried out from metacarbonate rocks and their surrounding pelitic schists, which is summarized below. 45 thin sections were examined under the microscope, corresponding to gradational contacts between garnet-bearing pelitic schists and metacarbonate layers (Figure 6) that have been observed in the staurolite-kyanite metamorphic zone of the Silgará Formation. Reaction bands of millimeter to centimeter scale display a complex mineralogy consisting of garnet, amphibole, diopside, quartz, plagioclase, ilmenite, titanite, rutile, epidote, clinozoisite, zoisite, calcite and dolomite. Mineral abbreviations after Kretz (1983). Quartz, plagioclase and minor potassium feldspar occur concentrated as layers as well as disseminated throughout the reactions zones. Biotite is present as discrete crystals, in discontinue lepidoblastic bands, concordant or sometimes discordant to the lithologic contacts. Muscovite is rarely observed as discrete

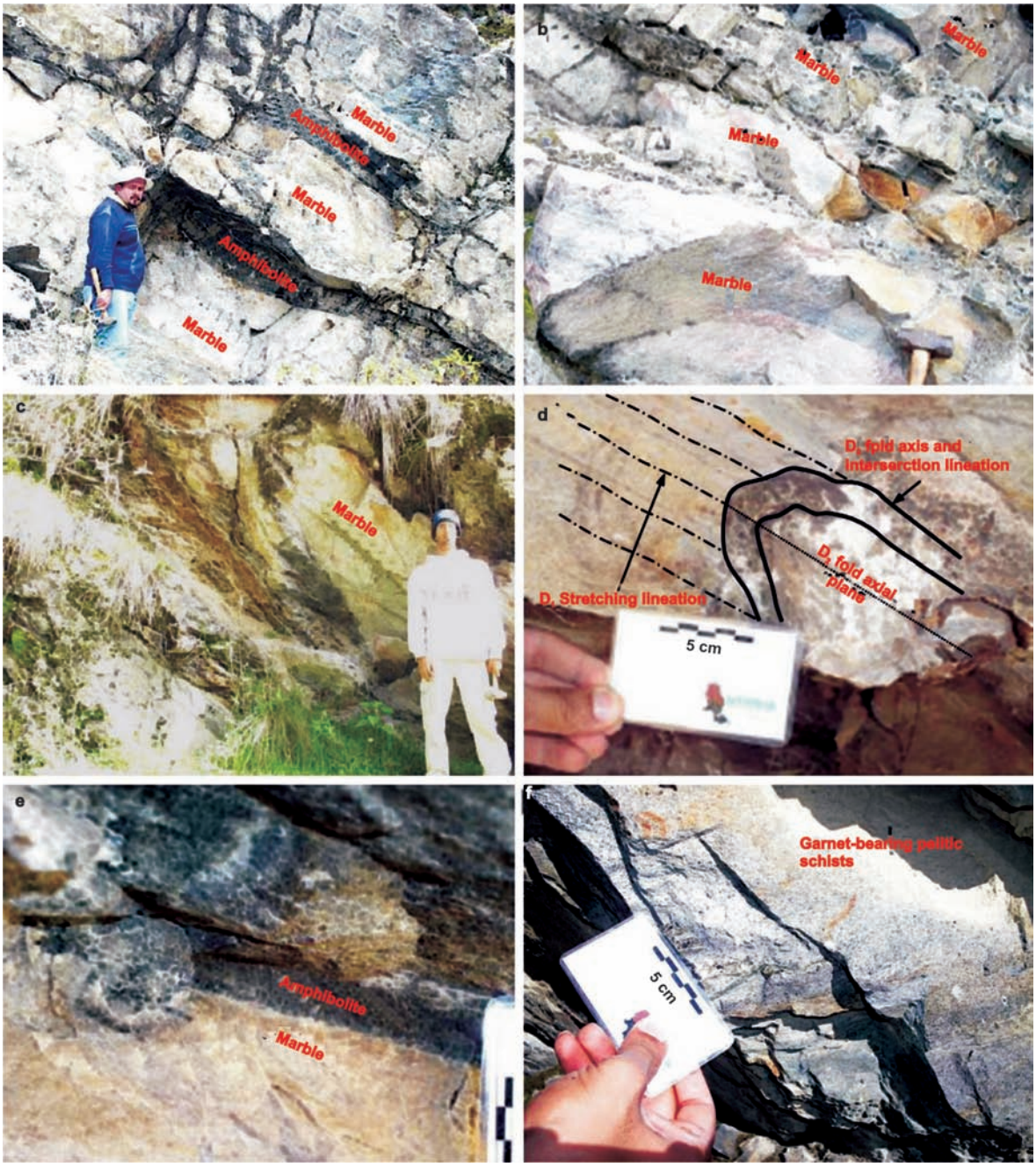

Figure 2. Field photographs of metacarbonate and related rocks at the central Santander Massif. (a) Outcrop from the Curpagá marble quarry in which marble and amphibolite are interlayered with pelitic schists. The foliation of the marble parallels that in the adjacent well-foliated pelites. (b) Close-up of (a) in which is observed a banded white, pink and gray marble up to 1 m of thickness interlayered with amphibolite within pelitic schists, developing calc-silicate reaction bands. (c) White marble with a lenticular geometry and up to 1 m of thickness interlayered with dark green banded amphibolite layers. (d) Recumbent fold (with a subhorizontal axial plane strikes N40ºW and dipping 25ºNE) in marble interlayered with pelitic schists where the way Mutiscua-Sucre cut the Valegrá stream. (e) Net contact between dark green amphibolite (upper part) and orange marble (lower part). (f) Breccia development in pelitic schist layers.

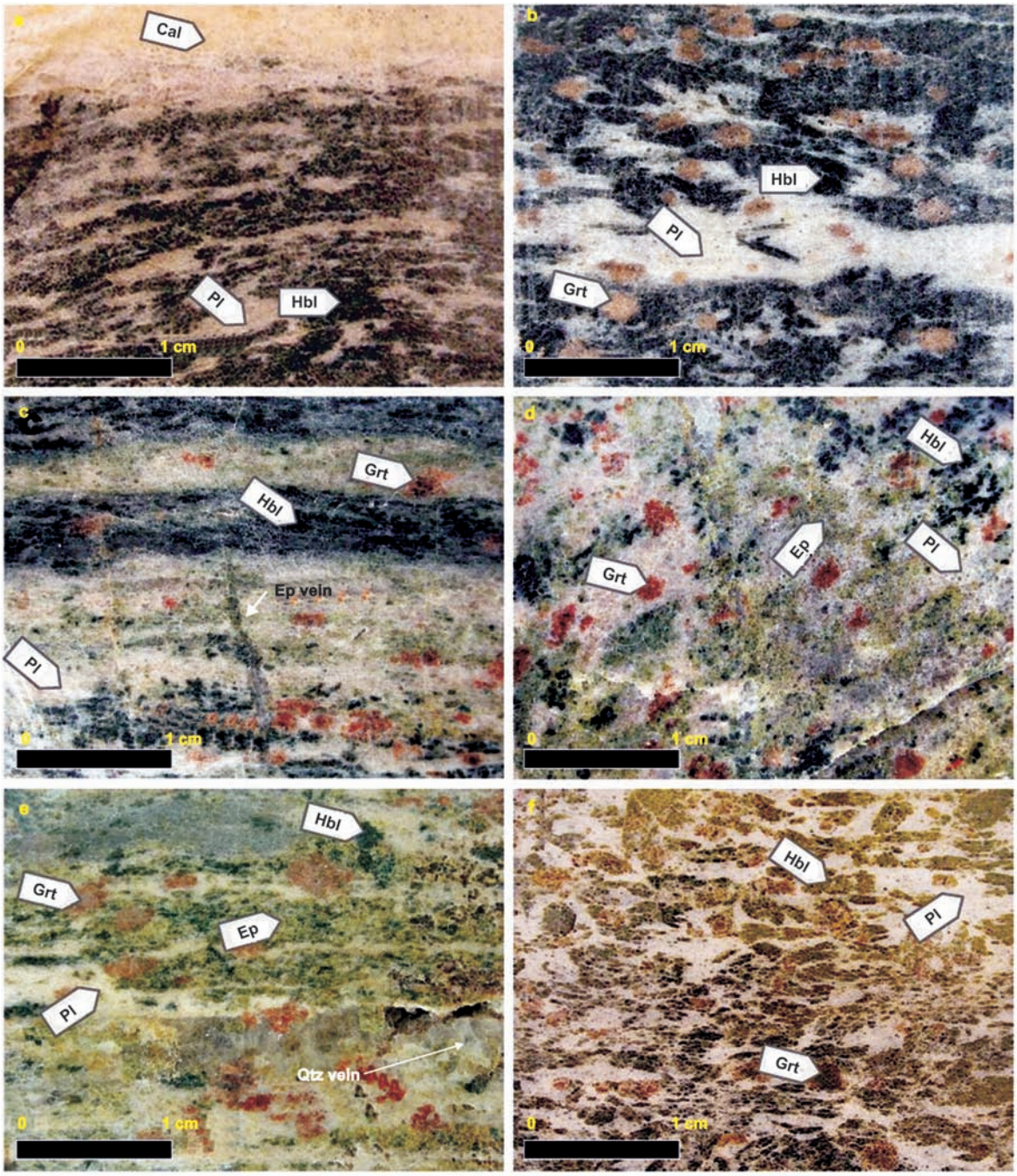

Figure 3. Photographs of hand specimens of different metacarbonate and related rocks interlayered within pelitic rocks of the Silgará Formation. Note the sharp change in the distribution of minerals at the boundary of zones. (a) Contact between a massive marble (at upper part) and a banded Zo-Czo-Act-bearing amphibolite (at lower part); sample RCS-16, (b) banded Amp-Grt-bearing calc-silicate rock; sample RCS-31, (c) banded, (d) massive and (e) banded Di-Amp-Grt-bearing calc-silicate rocks; samples RCS-38, RCS-36 and RCS-37, respectively, (f) Amp-Bt-Grt-bearing calc-silicate rocks; sample RCS-21.

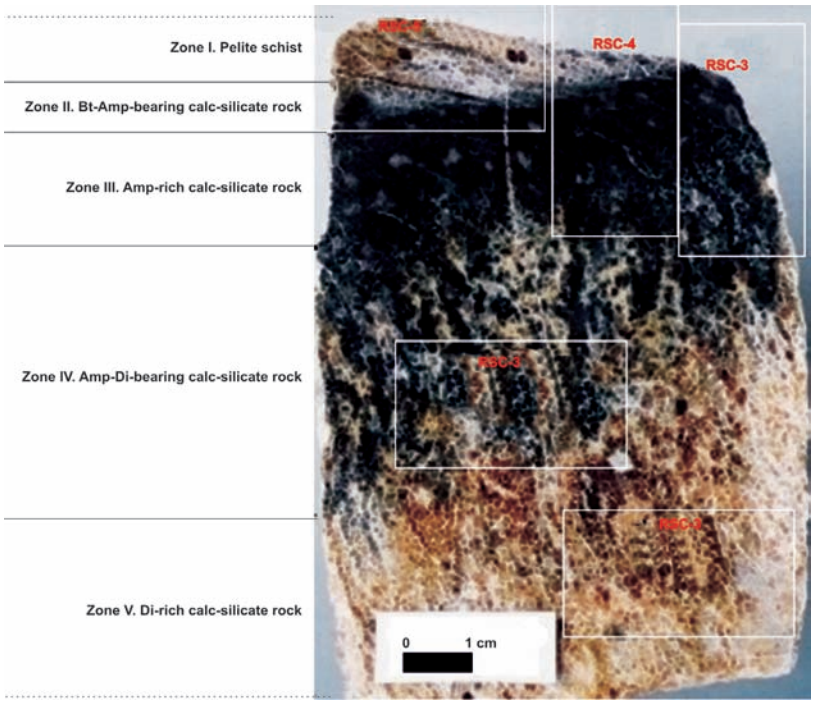

Figure 4. Photograph of a polished slab, showing the distribution of five thin sections (samples RCS-1,2,3,4 and 5) respect to the reaction zones between a garnet-bearing pelitic schist (at upper part) and marble (missing from sample at lower part), which show gradational contacts. The constituent minerals of the rock tend to be arranged almost perpendicular to the main foliation and across the lithologic contact between pelitic schist and marble. The following are the reaction zones identified from upper part to lower part: Zone I. Pelite schist; Zone II. Bt-Amp-bearing calc-silicate rock; Zone III. Amp-rich calc-silicate rock; Zone IV. Amp-Di-bearing calc-silicate rock; Zone V. Di-rich calc-silicate rock.

crystals only in pelitic schists. Garnet with a poiquiloblastic and skeletal character usually appears in all reaction zones, whereas sector-zoning garnet is found in quartz-rich bands of pelitic schists. Poiquiloblastic garnet contains quartz, plagioclase and ilmenite as the main inclusions, giving it a spongy appearance, which show a concordant relationship with the regional foliation or a randomly distribution and orientation. Skeletal garnet corresponds to large web-like garnet crystals containing so many quartz inclusions that the quartz predominates, and can be associated to very fast growth between quartz grain boundaries (Ríos *et al.*, 2003a). Garnet also occurs as xenoblastic relicts irregularly distributed in the reaction zones.

Amphibole (Fe-hornblende and actinolite) occurs as prismatic crystals, usually elongate, which displays pale green-to-green color and weak pleochroism, cross sections with two traces of exfoliation at 56 or 124°, and Carlsbad twinning. It occurs as crystals with a preferred orientation, although also as randomly oriented, large, poiquiloblastic and post-tectonic porphyroblasts that overgrew the main fabric of the rocks, containing inclusions of quartz, plagioclase and ilmenite. Clinopyroxene (diopside) occurs as prismatic, and less commonly, rounded or corroded crystals, which show slightly green color, high relief and bright first order birefringence colors, and two sets of cleavages at right angles to one another, although most of the crystals display at least one cleavage. Calcite is the common carbonate in the metacarbonate rocks, with minor amounts of dolomite. Epidote-group minerals occur in the matrix and as a secondary mineral phase, and they sometimes develop intergrowths with amphibole. Accessory minerals are

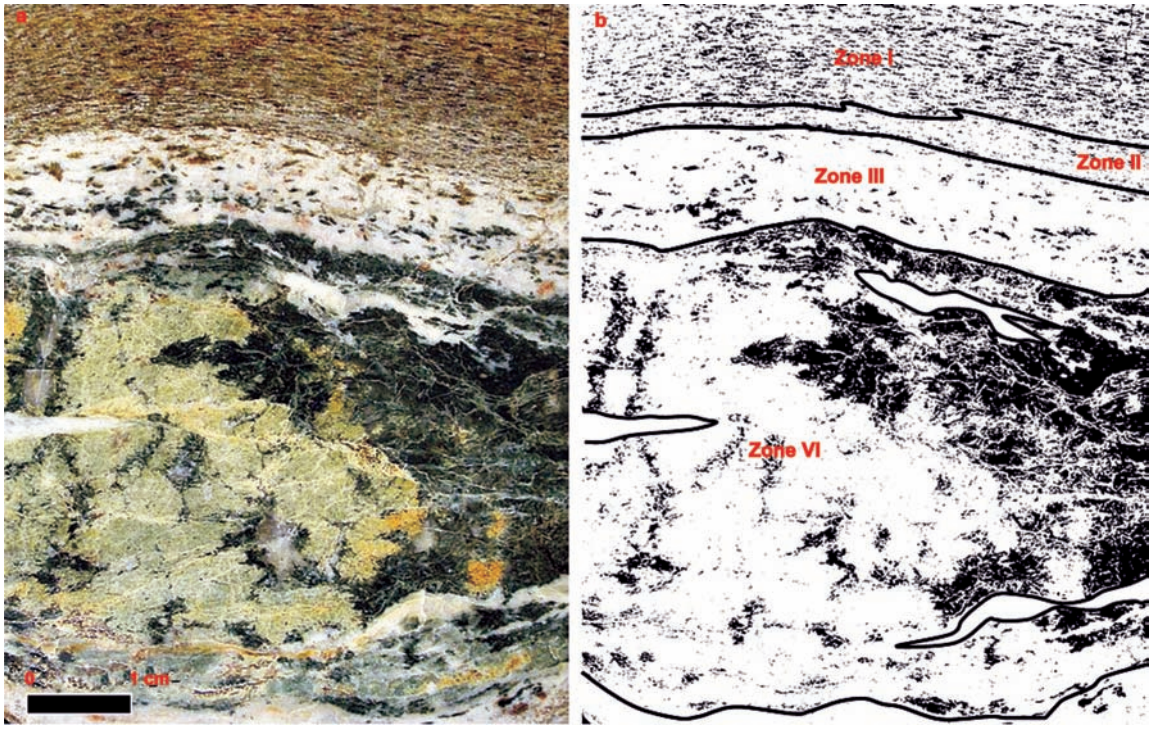

Figure 5. Photograph of a polished slab (sample RCS-29), left, and schematic diagram, right, of a profile across metacarbonate layers perpendicular to lithologic contacts with a pelitic schist, showing spatial distribution of mineral assemblages of metasomatic zones. Note the sharp change in the distribution of minerals at the boundary of zones. The following are the reaction zones identified from upper part to lower part: Zone I. Pelite schist. Zone II. Bt-Amp-bearing schist. Zone III. Bt-Amp-bearing calc-silicate rock. Zone IV. Amp-Di-bearing calc-silicate rock. (from Gómez y Avila, 2006).

zircon, apatite, tourmaline, ilmenite, titanite, rutile and graphite. Mineral assemblages in metacarbonate rocks change systematically with increasing metamorphic grade (Fritts, 1965; Hewitt, 1973; Palin, 1992; Ague, 2002). We document progressive changes in mineral assemblage zones in these rocks, although the regional distribution of assemblages has not yet been mapped. However, the isograds apparently were deflected by the presence of structural features, such as faults, that may have distorted the fluid flow paths. Campos (1999) reported the occurrence of a metasomatism zone between pelitic and marble layers, carrying out a textural and structural as well as mineralogical characterization. However, he did not define and characterize in detail different reaction zones as Gómez y Avila (2006) proposed and we synthesize in this study. Based on mineral assemblages and spatial distributions of mineral phases different reaction zones have been characterized were identified (Table 1). The arrangement of mineral phases in these metasomatic zones is usually parallel to the main foliation and the lithologic contact between pelitic schists and marble. If reaction progress varies across individual layers, it is greatest at lithologic contacts with surrounding metapelitic rocks or in reaction selvages around syn-metamorphic veins (Hewitt, 1973). Campos (1999) describes the occurrence of veins mainly composed of quartz with minor calcite in the metasomatic zones, suggesting a remo- bilization of SiO_2 and CaO due to the action of late magmatic fluids associated to the emplacement of granitic intrusives. The most complete sequence of metasomatic reaction zones that can be distinguished was observed in sample RCS-1-5, which corresponds to a calc-silicate rock near to a

Table 1. Prograde mineral assemblages. Reaction zones: Zone I. Grt-bearing pelite schist; Zone II. Bt-Amp-bearing calc-silicate rock; Zone III. Amp-rich calc-silicate rock; Zone IV. Amp-Di-bearing calc-silicate rock; Zone V. Di-rich calc-silicate rock; Zone VI. Ep+Czo+Zo-bearing calc-silicate rock; Zone VII. Marble. Rock types: DG, Di-Grt calc-silicate rock; DAG, Di-Amp-Grt calc-silicate rock; AG, Amp-Grt calc-silicate rock; ABG, Amp-Bt-Grt calc-silicate rock; GP, Grt-bearing pelitic schist; AS, St-bearing amphibolite; P, pelitic schist; AB, Amp-Bt calc-silicate rock; A, amphibolite; DA, Di-Amp calc-silicate rock; M, marble; EG, Ep-group-bearing calc-silicate rock. Mineral abbreviations after Kretz (1983).

Sample	Zone	Type	Cal	Dol	Qtz	Pl	Kfs	Bt	Ms	Grt	St	Amp	Di	Scp	Ep	Czo	Zo	Ilm	Ttn	Rt
RCS-1	V	DG			■	■	■			■			■	■					■	■
RCS-2	IV	DAG			■	■	■			■		■	■	■			■		■	
RCS-3	II	AB			■	■		■				■						■	■	
RCS-3	III	AG			■	■				■		■						■	■	
RCS-4	I	GP			■	■		■		■								■		
RCS-4	II	ABG			■	■		■		■		■						■	■	
RCS-5	I	GP			■	■		■		■								■		
RCS-5	II	ABG			■	■		■		■		■						■	■	
RCS-7	IV	DAG	■		■	■				■		■	■				■		■	
RCS-8	III	AS			■	■		■			■	■						■		
RCS-9	I	P			■	■		■										■	■	
RCS-9	II	AB			■	■		■				■						■	■	
RCS-9	III	A			■	■						■						■	■	
RCS-13	III	AG			■	■				■		■			■		■		■	
RCS-15	II	AB			■	■		■				■			■				■	
RCS-15	III	A	■		■	■						■			■	■			■	
RCS-15	IV	DA	■									■	■		■	■			■	
RCS-16	III	A	■	■								■				■	■		■	
RCS-16	VII	M	■	■																
RCS-19	I	P			■	■		■										■	■	
RCS-19	II	AB			■	■		■				■						■	■	
RCS-21	II	ABG			■	■		■		■								■		
RCS-25	III	AG			■	■				■		■			■		■	■	■	
RCS-29	I	GP			■	■		■		■								■		
RCS-29	II	ABG			■	■		■		■		■						■	■	
RCS-29	III	A			■	■						■						■	■	
RCS-29	IV	DAG			■	■				■		■	■	■			■		■	
RCS-31	III	AG			■	■				■		■						■	■	
RCS-34	III	AG			■	■				■		■			■	■	■		■	
RCS-35	I	GP			■	■		■	■	■								■		
RCS-35	III	AG			■	■				■		■							■	
RCS-35	IV	DAG	■		■	■				■		■	■				■		■	
RCS-36	I	P	■		■			■	■											
RCS-36	IV	DAG			■	■				■		■	■			■	■		■	
RCS-37	III	A	■		■	■						■	■			■	■		■	
RCS-37	IV	DAG	■		■	■				■		■	■				■			
RCS-38	IV	DAG	■		■	■				■		■	■			■	■		■	

quartz vein, and the reaction zones are due to the interaction between sector-zoned garnet-bearing pelite and calcite marble layers. The metasomatic reaction zones defined in this study are similar to those described by other researchers (e.g., Thompson, 1975; Kerrick, 1977; López and Soto, 1999).

Zone I (garnet-bearing pelitic schist) shows a well developed schistosity and is characterized by the presence of sector-zoned garnet, associated to quartz, plagioclase and biotite, with accessory zircon, apatite, tourmaline, ilmenite, calcite and muscovite. Garnet can be also poiquiloblastic (with an inclusion patterns of quartz, plagioclase and ilmenite parallel to the main foliation of the rock) and skeletal. In the region next to the calc-silicate zones muscovite or Al_2SiO_5 polymorphs do not occurs, which can be due to process of diffusion. The mineral assemblage in this zone is biotite + plagioclase ± K-feldspar ± garnet.

Zone II (biotite-amphibole-bearing calc-silicate rock) corresponds to the interface between zones I and III and marks the abruptly appearance of amphibole (Fe-hornblende or actinolite) with biotite

remnants, which show the same orientation as the amphibole and in some case intergrowths between biotite and amphibole, which are associated to garnet. It is characterized by a decrease in biotite, as well as drastically decreases of quartz and plagioclase. Accessory mineral phases are ilmenite and titanite, the latest developing pseudomorphs after ilmenite. Epidote-group minerals also occur in this region. This reaction zone is defined by the occurrence of traces of brownish-orange biotite and ubiquitous pale green hornblende in equilibrium with garnet as bands with a nematoblastic texture. The mineral assemblage in this reaction zone is quartz + plagioclase + biotite + hornblende + garnet + titanite + zircon + apatite + ilmenite (calc-silicate rock). There is an unusual mineral assemblage characterized by quartz + plagioclase + biotite + hornblende + staurolite, with accessory ilmenite and tourmaline.

Zone III (amphibole-rich calc-silicate rock) exhibits a foliated granonematoblastic fabric, and is defined by the disappearance of brownish-orange biotite and the ubiquitous occurrence of pale green amphibole (Fe-hornblende or actinolite) in equilibrium with garnet. Garnet is poiquiloblastic (with an inclusion pattern of quartz and plagioclase parallel to the main foliation of the rock) and skeletal. It also contains quartz, plagioclase and epidote-group minerals, with accessory ilmenite, titanite, calcite and dolomite. The mineral assemblage in this zone is plagioclase + amphibole ± garnet ± epidote.

Zone IV (amphibole-diopside-bearing calc-silicate rock) is characterized by a weakly foliated granoblastic fabric, which is dominated by coarse-grained clinopyroxene (diopside) followed in modal abundance by amphibole. It shows the abruptly appearance of diopside and zoisite and a decrease of the amphibole, and is characterized by the occurrence of the highest amount of diopside, and garnet tends to disappear. Garnet is poiquiloblastic (with inclusions of quartz, zoisite and calcite) or skeletal, and can be replaced by zoisite and calcite or uncommonly by quartz, calcite, diopside and amphibole, developing pseudomorphs. There is a regular intergrowth between amphibole (Fe-hornblende or actinolite) and diopside, which are associated to quartz, plagioclase, garnet, epidote-group minerals (mainly zoisite), calcite and titanite. Abundant coarse titanite crystals are very common in this zone. It is usual to observe quartz + zoisite ± calcite within this zone. In some cases, actinolite probable formed after diopside. Scapolite occurs as poiquiloblasts, which show inclusions of diopside, quartz, titanite and calcite. The mineral assemblage in this zone is amphibole + diopside + garnet + plagioclase.

Zone V (diopside-rich calc-silicate rock), not yet directly in contact with marble (Zone VII), displays a granoblastic fabric, which is characterized by a high content of clinopyroxene (diopside). Diopside usually occurs as poiquiloblasts crowded with inclusions of amphibole, quartz, titanite and calcite or as massive bands, and it sometimes is overgrown by amphibole in the border, can be partially or completely altered to a very fine-grained mass of chlorite, other sheet silicates, and calcite. In these cases, diopside and plagioclase abundance are inversely related. More rarely, small diopside grains also appear in contact with plagioclase and amphibole. Quartz is only rarely in contact with calcite and is usually found in the core of diopside. Subvertical fractures that connect calc-silicate layers with calcareous layers are commonly observed, as are diopside-filled fractures. The diopside can represent a mineral phase produced by the reaction of quartz + dolomite (e.g., Thompson, 1975; Robinson, 1991). It is probable that this reaction proceeds until one of the dolomite was consumed, which can be due to condition of extremely high X_{CO2} in the marble. However, Nabelek (2002) considers that the dominant diopside-forming reaction may have been phlogopite + quartz + calcite = diopside + microcline + CO_2 + H_2O. In a Fe-present system, the stability field of tremolite is reduced (Nabelek, 2002). Therefore, this can explain why tremolite was not observed in the examined rocks, taking into account that this mineral is much more common in magnesium-rich systems. Scapolite appears within bleached calc-silicate layers of the diopside-rich zone as small grains in contact with diopside, amphibole, plagioclase, titanite and calcite. The scapolite-forming reaction is often described in

terms of the calcium anorthite and meionite end-members as anorthite+calcite = meionite (Nabelek, 2002). This end-member reaction is vapor-absent and occurs at approximately 800ºC (Moecher & Essene, 1990). Although thermodynamic data for the sodium end-member of scapolite, marialite, are lacking, empirical observations suggest that the stability field of scapolite expands to lower temperatures with introduction of the marialite component (Mora & Valley, 1989; Oliver *et al.*, 1992). Indeed, the occurrence of scapolite within this reaction zone suggests that it formed at approximately 500ºC (Nabelek, 2002).

Zone VI (epidote-clinozoisite-zoisite-bearing calc-silicate rock), the boundary between zones V and VII, is characterized by the occurrence of epidote-group minerals along with quartz and accessory titanite and calcite, with no garnet.

Zone VII (marble) shows a granoblastic-polygonal texture and consists of recrystallized coarse calcite and minor dolomite. Wollastonite or scapolite was not identified in the analyzed marble samples. The mineral assemblage in this zone is calcite ± dolomite

Mineral Chemistry

Electron microprobe analyses were performed using a JEOL JXA 8800M electron microprobe analyzer of the Department of Geosciences at Shimane University, under the following analytical conditions: accelerating voltage and specimen current are 15 kV and $2.0x10^{-8}$ Å, respectively. Data acquisition and reduction were performed using the correction method of Bence & Albee (1968), using natural and synthetic minerals as standards. Electron backscatter diffraction analyses of a calc-silicate rock, which contains the defined reaction zones, were performed by Dr. Alan Boyle from the Microstructure Research Group of the Department of Earth & Ocean Sciences at the University of Liverpool (England), using an Electron Backscatter Diffractometer (EBSD) Philips XL30 SEM, Oxfords Instruments Isis X-ray Analysis System, under the following analytical conditions: accelerating voltage 20 Kv and spot size 5.5 (~0.9 nA); 80 second real-time counting with around 20-25% dead time. Data acquisition and reduction were carried out using the ZAF correction method, using natural mineral and pure metal standards (Si-Wollastonite, Al-Corundum, Fe-Metal, Ti-Metal, Mn-Metal, Mg-Periclase, Ca-Wollastonite, Na-Albite, and K-Orthoclase). Mineral compositions were determined by multiple spot analyses. The Ca-amphibole formulae were calculated on an anhydrous basis to a total of 13 cations, excluding Ca, Na and K, per 23 atoms of oxygen, using the charge-balance method to assign ferrous and ferric iron, and the cations assigned to each site according to IMA guidelines (Leake, 1978). Representative analyses and chemical formulas of the minerals are shown in Table 3.

Garnet displays normal, reversal or sector zoning in metapelitic rocks. Garnet usually shows a normal zoning pattern indicating prograde growth, with a strongly modified bell-shaped spessartine profile, increasing almandine and pyrope contents, and an overall gradual decrease in Fe/(Mg+Fe) from core to rim. All analyzed garnets exhibit chemical zoning. In general, garnet is almandine-rich ($Alm_{72-70}Sps_{1-1}Prp_{15-15}Grs_{12-14}$), including the sector-zoned garnet ($Alm_{75-89}Sps_{4-0}Prp_{4-11}Grs_{17-11}$) in pelites close to quartz veins in calc-silicate rocks, which contain grossular-rich garnet ($Alm_{60-41}Sps_{12-9}$ $Pr_{7-4}Grs_{21-46}$). Chemical compositions of analyzed garnet from pelitic and metacarbonate and related rocks are listed in Tables 1-3 and illustrated in Figure 9.

Staurolite is Fe-rich (X_{Fe} = 0.68-0.89), but does not show any zonation in Fe and Mg. A representative chemical data of staurolite is presented in Table 2. Castellanos (2001) reported up to 3.70 weight % of ZnO in staurolite, but it shows homogeneous Zn distribution.

Clinopyroxene is essentially a diopside-hedenbergite solid solution. Representative chemical compositions of the analyzed clinopyroxene are listed in Table 3 and plotted in Figure 8. The end-member components were calculated on the basis of Essene and Fyfe (1967) as follows: jadeite (3.64-3.76 %), acmite (0.00 %), and augite (96.36-96.24 %). The

Table 2. Representative mineral analyses of the metacarbonate and associated rocks in the central Santander Massif (data from Castellanos, 2001)

Rock type	A	A	A	A	A	A	A	A	A	A	A	A	A	A	A	A	A	A	M	A
Sample	PCM-28	PCM-128	PCM-28	PCM-128	PCM-138	PCM-28	PCM-31	PCM-128	PCM-138	PCM-28	PCM-31	PCM-31	PCM-28	PCM-138	PCM-28	PCM-31	PCM-138	PCM-128	PCM-31	PCM-138
Mineral	Grt	Grt	Fe-Ts	Mg-Hbl	Fe-TS	Pl	Pl	Pl	Pl	Ms	Ms	Chl	Ep	Czo	Ttn	Ttn	Ttn	Rut	Cal	Cal
Analysis	12 (rim)	1 (rim)	1	1	6	1	8	3	1	1	1	6	3	7	2	1	1	2	5	1
SiO_2	37,27	37,63	43,35	46,17	42.25	46,60	62,10	45,04	61,69	46,38	47,46	27,68	37,88	38,14	30,62	29,01	29,60	0,03	0,00	0,00
TiO_2	0,04	0,07	0,38	0,46	0,46	0,00	0,00	0,00	0,00	0,00	0,17	0,09	0,11	0,20	34,26	37,85	37,87	98,51	0,00	0,01
Al_2O_3	21,40	21,59	13,18	12,10	13,59	34,50	23,06	35,36	23,43	35,00	29,72	20,08	30,25	28,37	3,34	1,90	2,42	0,09	0,00	0,00
FeO	31,42	22,12	19,92	11,84	19,29	0,87	0,31	0,09	0,19	1,27	3,66	15,84	6,04	5,45	0,38	1,05	0,31	1,12	0,36	1,10
MnO	1,06	7,60	0,25	0,52	0,18	0,01	0,00	0,00	0,03	0,00	0,00	0,08	0,09	0,04	0,14	0,04	0,02	0,20	0,10	0,31
MgO	3,78	3,46	7,81	7,81	7,93	0,20	0,13	0,00	0,10	0,59	1,90	21,66	0,04	0,07	0,02	0,00	0,00	0,01	0,63	0,42
CaO	5,09	6,40	11,64	11,64	11,79	12,46	2,14	18,20	2,86	0,02	0,16	0,08	23,90	23,52	29,47	27,77	27,64	0,13	52,42	54,71
Na_2O	0,04	0,00	0,69	0,69	0,89	1,14	7,87	1,09	7,75	0,02	0,19	0,00	0,00	0,00	0,06	0,05	0,00	0,01	0,00	0,03
K_2O	0,05	0,03	0,36	0,36	1,10	3,44	1,65	0,07	3,22	11,94	10,70	0,09	0,06	0,06	0,02	0,02	0,05	0,02	0,00	0,04
Total	100,16	98,88	97,58	97,58	97,49	99,21	97,27	99,83	99,27	95,23	93,97	85,61	98,36	95,86	98,31	97,69	97,90	100,12	53,51	56,62
Oxygen basis	12	12	23	23	23	8	8	8	8	22	22	28	25	25	5	5	5	2	6	6
Si	2,968	3,001	6,539	6,648	42,252	2,169	2,816	1,235	1,67	6,211	6,492	5,665	5,907	6,083	0,573	0,548	0,555	0,000	0,000	0,000
Ti	0,002	0,004	0,043	0,049	0,455	0,000	0,000	0,000	0,000	0,000	0,018	0,014	0,013	0,024	0,482	0,537	0,534	0,990	0,000	0,000
Al	2,008	2,029	2,343	2,053	13,591	1,893	1,232	1,143	0,748	5,525	4,790	4,844	5,558	5,332	0,074	0,042	0,054	0,001	0,000	0,000
Fe^{3+}	0,051	0,000	0,784	0,670	4,875	0,000	0,000	0,000	0,000	0,000	0,000	0,000	0,787	0,727	0,000	0,000	0,000	0,000	0,000	0,000
Fe^{2+}	2,041	1,475	1,729	0,777	14,907	0,871	0,012	0,002	0,004	1,272	0,419	2,711	0,000	0,000	0,006	0,0017	0,005	0,012	0,031	0,092
Mn	0,071	0,513	0,031	0,064	0,181	0,007	0,000	0,000	0,001	0,000	0,000	0,014	0,012	0,006	0,002	0,001	0,000	0,002	0,009	0,026
Mg	0,449	0,412	1,757	2,761	7,93	0,196	0,009	0,000	0,004	0,591	0,388	6,0609	0,009	0,017	0,000	0,000	0,000	0,000	0,097	0,062
Ca	0,434	0,546	1,881	1,791	11,788	12,455	0,104	0,535	0,083	0,022	0,024	0,018	3,992	4,019	0,59	0,562	0,556	0,002	5,854	5,813
Na	0,014	0,000	0,203	0,250	0,890	1,142	0,692	0,058	0,407	0,021	0,05	0,000	0,000	0,000	0,002	0,002	0,000	0,000	0,000	0,006
K	0,011	0,006	0,069	0,051	1,104	3,439	0,096	0,002	0,111	11,941	1,867	0,025	0,012	0,012	0,000	0,001	0,001	0,000	0,000	0,005
Total	8,049	7,986	15,379	15,113	97,973	22,172	4,961	2,975	3,028	25,583	14,048	19,899	16,290	16,220	1,730	1,708	1,705	1,009	5,992	6,005
X_{Mg}	0,18	0,22	0,50	0,78	0,35					0,32	0,48	0,71			0,07	0,00	0,00	0,02		
X_{An}						0,92	0,21	0,94	0,27											
X_{Al}												1,00			0,13	0,07	0,09			
Al_2Fe %													18,12	17,91						

* X_{Al}= Al/(Al+Ti+Fe^{3+}); Al_2Fe%=Fetot/(Fetot+Al-2)*100; A, amphibolite; M, marble

Table 3. Representative chemical compositions of mineral phases from pelitic schists associated to metacarbonate rocks in the central Santander Massif (data from Castellanos, 2001).

Rock type	PS	PS	PS	PS	PS	PS	PS	PS	PS	PS	PS
Sample	PCM-28	PCM-28	PCM-28	PCM-28	PCM-28	PCM-618	PCM-618	PCM-618	PCM-618	PCM-618	PCM-618
Mineral	Grt	Grt	St	Bt	Pl	Grt	Grt	St	Bt	Ms	Pl
Analysis	1 (core)	13 (rim)	1	1	1	9 (core)	18 (rim)	4	10	7	3
SiO_2	36,96	36,87	27,55	35,70	59,48	36,54	37,34	26,55	35,00	47,69	58,31
TiO_2	0,03	0,04	0,61	1,41	0,00	0,07	0,02	0,52	2,51	0,70	0,00
Al_2O_3	21,64	21,40	53,74	18,56	25,89	20,48	20,76	54,48	18,63	35,82	25,28
FeO	33,83	32,32	13,63	18,35	0,03	34,23	36,18	13,19	20,73	1,06	0,28
MnO	0,47	0,48	0,00	0,00	0,00	1,73	0,16	0,01	0,01	0,00	0,00
MgO	3,79	3,70	1,76	11,91	0,00	0,91	2,62	1,21	8,09	0,58	0,01
CaO	4,24	4,87	0,00	0,01	6,62	5,94	3,52	0,00	0,00	0,00	7,03
Na_2O	0,01	0,00	0,00	0,47	7,83	0,02	0,00	0,08	0,46	0,82	7,62
K_2O	0,04	0,05	0,03	8,86	0,11	0,01	0,02	0,04	8,95	9,34	0,15
Total	101,02	99,73	97,32	95,28	99,96	99,93	100,62	96,09	94,38	96,02	98,68
Oxygen basis	12	12	23	22	8	12	12	23	22	22	8
Si	2,935	2,954	3,823	5,395	2,651	2,979	2,997	3,72	5,412	6,34	2,651
Ti	0,002	0,002	0,064	0,160	0,000	0,004	0,001	0,055	0,292	0,069	0,000
Al	2,025	2,021	8,788	3,306	1,36	1,968	1,963	8,995	3,396	5,518	1,341
Fe^{3+}	0,100	0,068	0,000	0,000	0,000	0,066	0,040	0,000	0,000	0,000	0,000
Fe^{2+}	2,146	2,097	1,582	2,319	0,001	2,267	2,389	1,545	2,68	0,116	0,011
Mn	0,032	0,032	0,000	0	0,000	0,119	0,011	0,001	0,001	0,000	0,000
Mg	0,449	0,442	0,364	2,683	0,000	0,111	0,313	0,253	1,866	0,113	0,000
Ca	0,361	0,418	0,000	0,001	0,316	0,519	0,303	0,001	0	0,000	0,339
Na	0,004	0,000	0,000	0,138	0,677	0,005	0,000	0,021	0,139	0,209	0,665
K	0,009	0,01	0,005	1,708	0,006	0,002	0,004	0,007	1,765	1,557	0,009
Total	8,063	8,044	14,626	15,711	5,011	8,04	8,021	14,579	15,55	13,816	5,016
X_{Mg}	0,17	0,17	0,19	0,54		0,05	0,12	0,14	0,41	0,49	
X_{An}					0,46						0,48

PS, pelitic schist

X_{Mg} ranges between 0.61 and 0.63, although it could change between different samples and also within the same sample as a consequence of a bulk-rock chemistry control. It shows very low contents of Al_2O_3 (0.92-1.11 wt %), TiO_2 (0.00-0.37 wt %), Na_2O (0.49 wt %) and MnO (0.44-0.45 wt %).

Amphibole structural formula calculation and classification were carried out according to Leake (1978). Representative analyses of amphibole are shown in Tables 2 and 4. Analyzed amphibole displays a wide range in chemical compositions, as illustrated in Figure 10a. The Si^{IV} ranges from 6.030 to

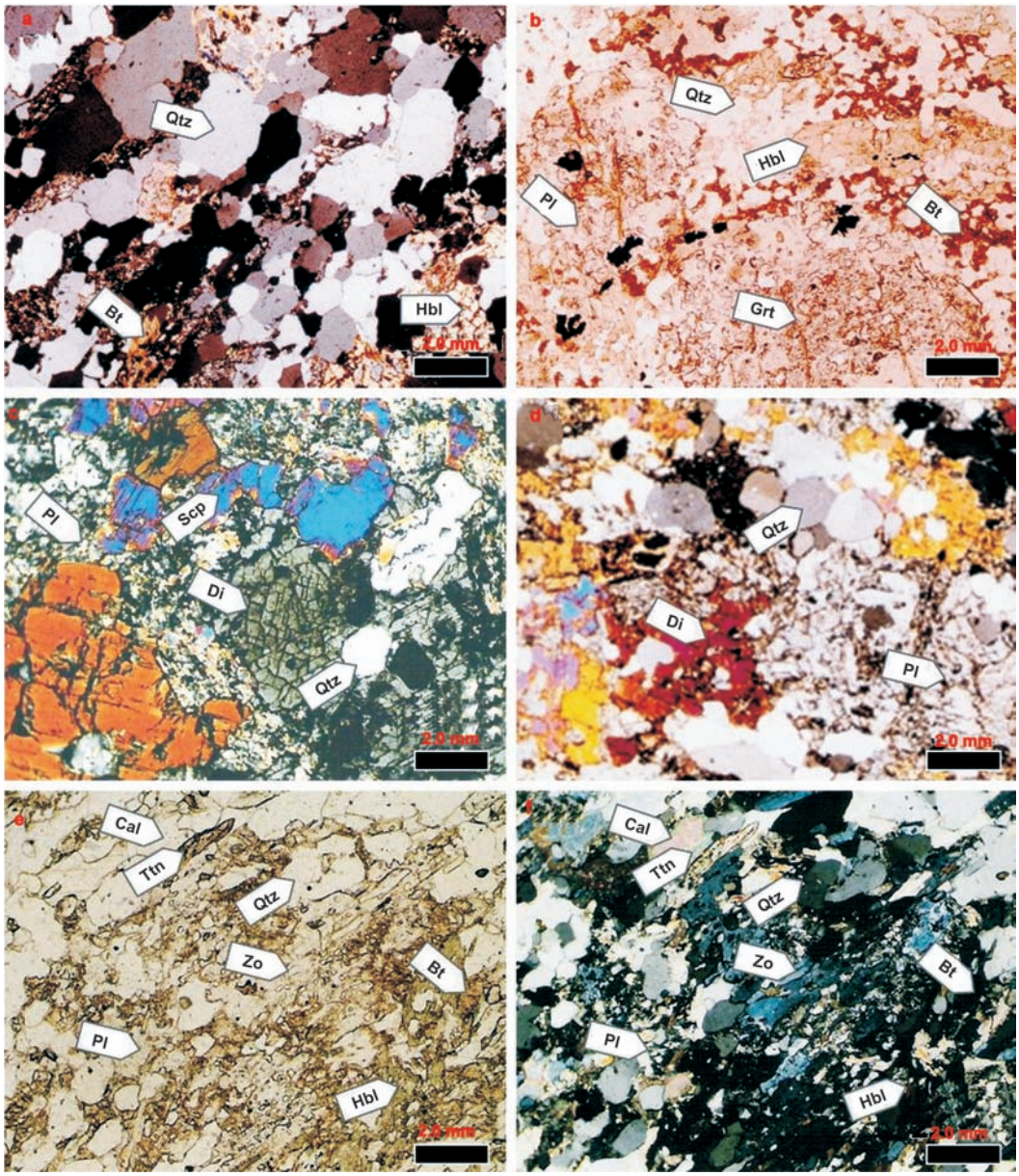

Figure 6. Photomicrographs of the main petrographic features observed in different calc-silicate rocks. (a) Quartz-rich reaction zone, in which biotite and amphibole are associated; cross-polarized light, 8x, RCS-2. (b) A textural sector-zoning garnet occurring in quartz-rich bands with other textural types of garnet (skeletal and poikiloblastic). This unusual zoning shows in general terms a radial character. The concentration of inclusions at interfacial boundaries gives spectacular sector-zoning garnet porphyroblasts, which display asymmetrical pressure shadows consisting mainly of quartz and biotite around them; plane-polarized light, 8x. (c) Diopside crystals, associated to quartz and plagioclase strongly altered to sericite. Diopside is recognized by its characteristic cleavage in two directions about 90°, high relief, as well as first and second order interference color; cross-polarized light, 8x, RCS-1. (d) Typical association of diopside, quartz and plagioclase (strongly sericitized); cross-polarized light, 8x, RCS-1. (e) and (f) phomicrographs in plane and cross-polarized light, respectively of a calc-silicate rock, which illustrate the occurrence of zoisite, associated to quartz, plagioclase, hornblende, calcite and titanite. Zoisite shows a short prismatic form, high relief, anomalous interference colors irregularly distributed and straight extinction; 8x, RSC-6.

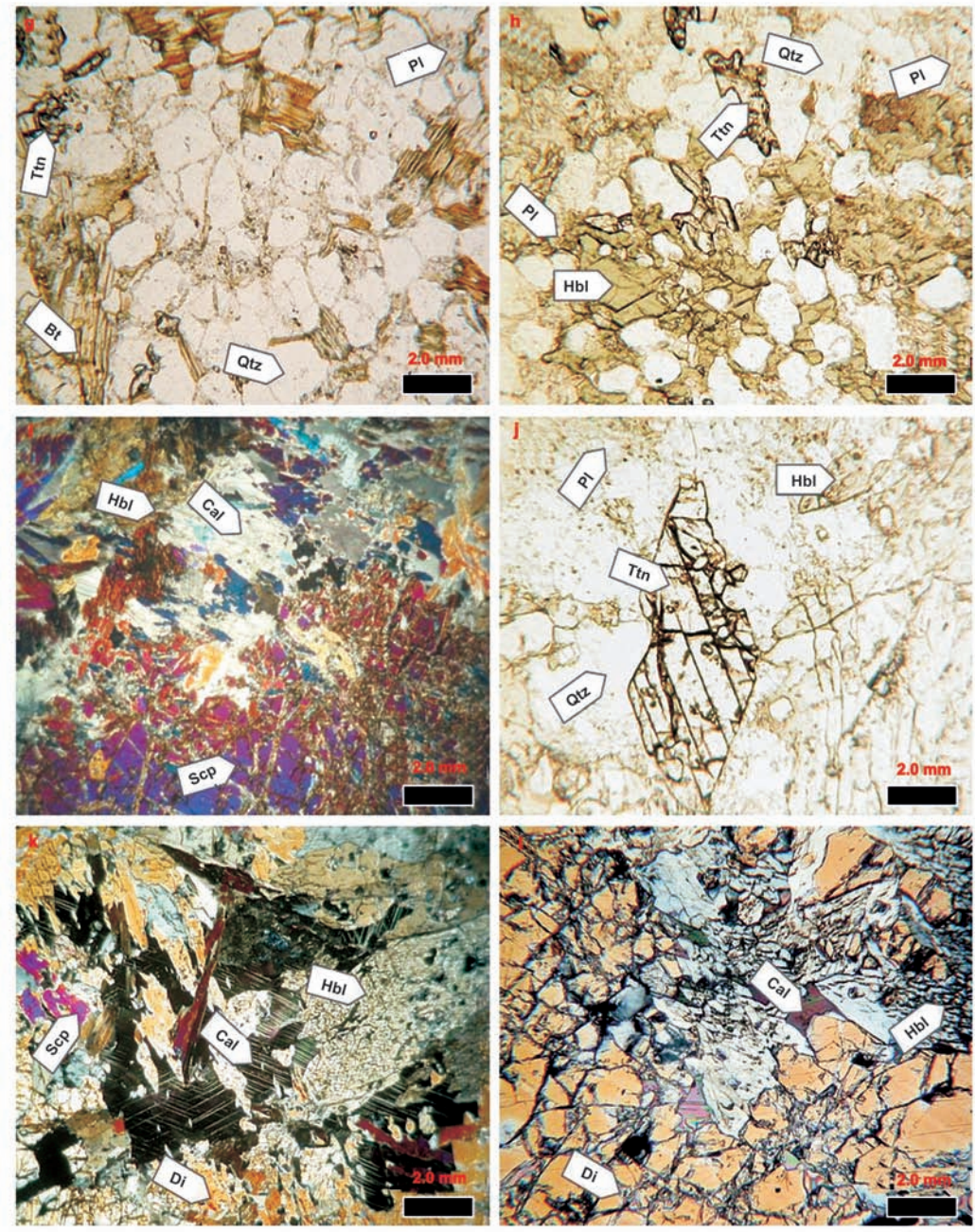

Figure 6 (continuation). Photomicrographs of the main petrographic features observed in calc-silicate reaction zones of the sample RCS-29, in which can be distinguished the distribution of the occurring mineral phases from the pelitic zone to the marble zone. (g) Occurrence of randomly oriented crystals of biotite partly replaced by chlorite in a pelitic zone; plane-polarized light, 8x. (h) Appearance of amphibole in the contact between the previous zone and a amphibole-rich zone; plane-polarized light, 8x. (i) Occurrence of a highly fractured scapolite crystal highly partially replaced by calcite and associated to amphibole; cross-polarized light, 8x. (j) Enormous crystal of titanite occurrence in a reaction zone, close to the diopside zone. (k) Transitional zone in which is observed the occurrence of amphibole, diopside and calcite; cross-polarized light, 8x. (l) Occurrence of a highly amount of diopside, with amphibole and minor calcite; cross-polarized light, 8x.

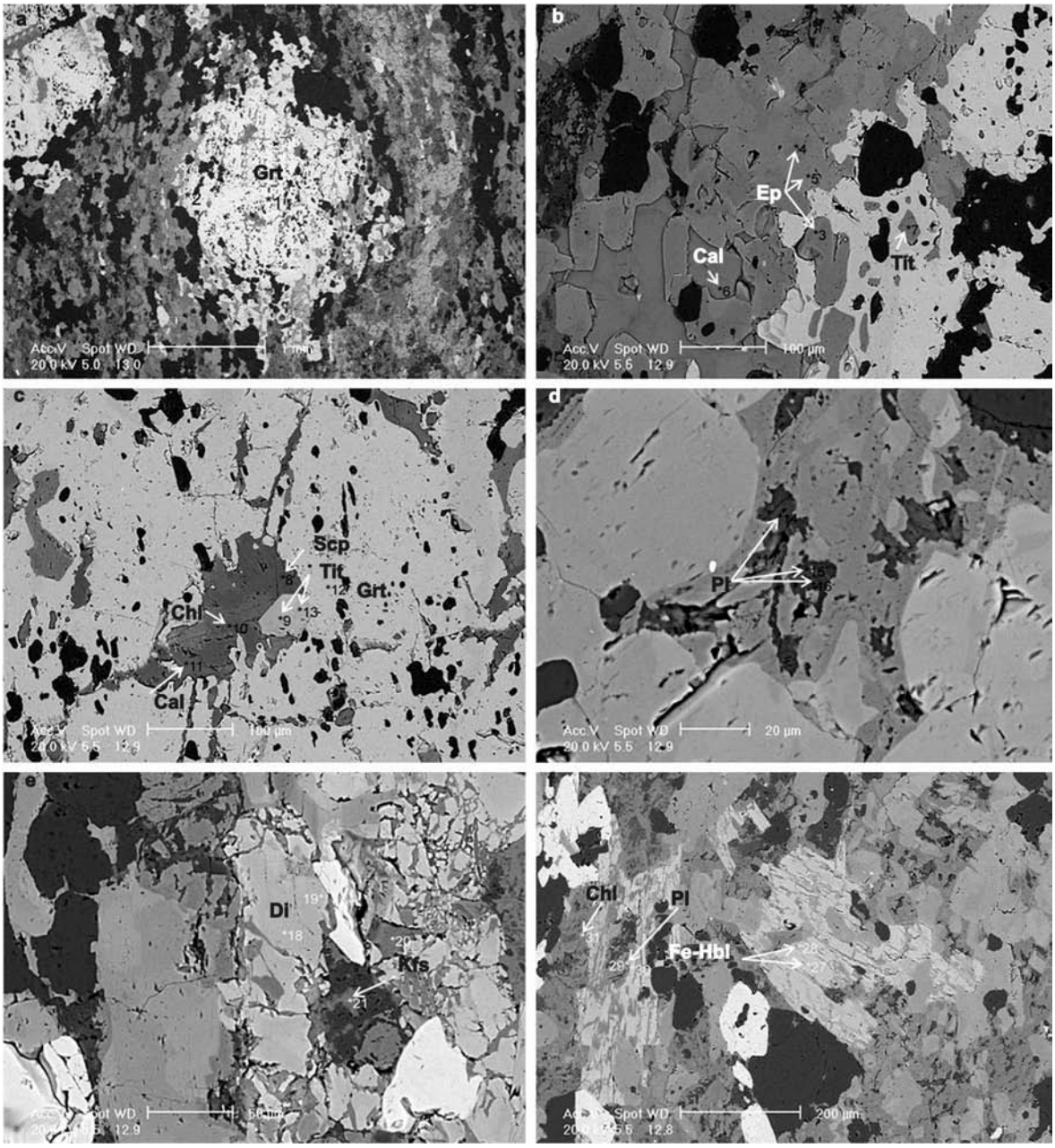

Figure 7. Back-scattered electron microscope (BSE) images of a calc-silicate rock (RSC-2) of the Silgará Formation, showing analytical points (see Table 3) of mineral phases, and the occurrence of (a) sector zoned garnet (1,2); (b) zoned epidote (3,4,5), calcite (6), titanite (7); (c) scapolite (8), garnet (12), titanite (9,13), chlorite (10) and calcite (11); (d) plagioclase (14,15,16); (e) diopside (18,19), and K-feldspar (21); (f) Fe-hornblende (27,28), plagioclase (29) and chlorite (31).

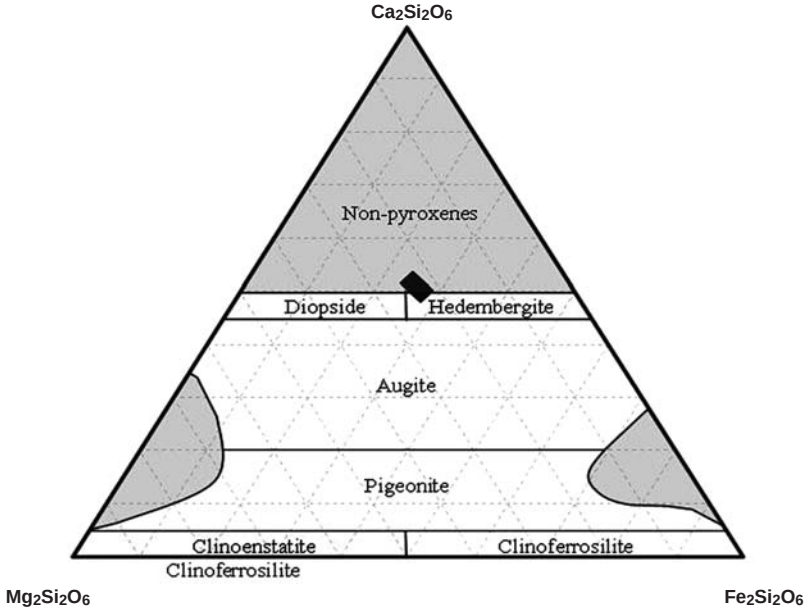

Figure 8. Wo-En-Fs triangular plot, showing the composition and nomenclature. Analyzed pyroxene from a calc-silicate rock reported in this study is indicated by black rhombs.

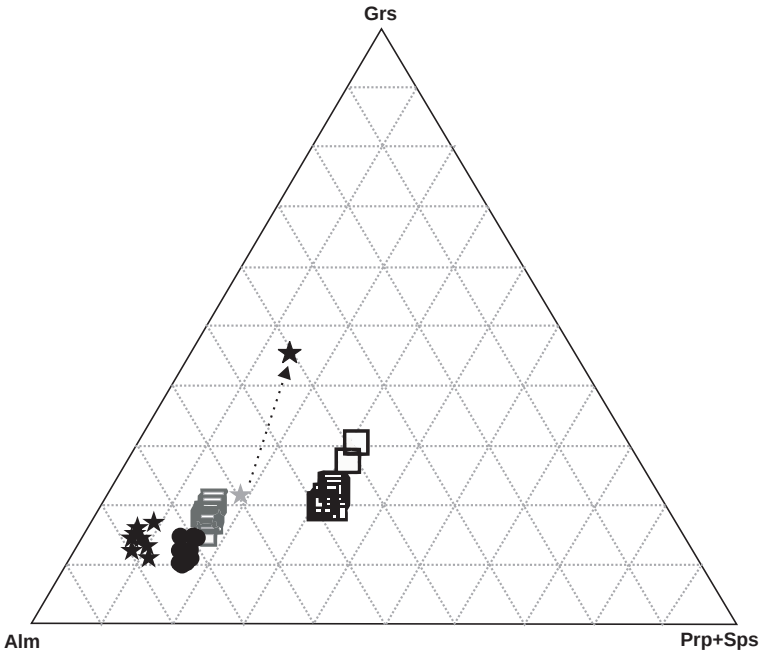

Figure 9. Chemical compositions of garnet expressed in an Alm-Grs-Prp+Sps diagram. Arrow indicates the compositional trend from core to rim in garnet-bearing samples. Symbols correspond to garnet-bearing amphibolite (PCM-128), open black squares; garnet-bearing amphibolite in contact with pelitic schist (PCM-28), open grey squares; garnet-bearing pelitic schist in contact with amphibolite (PCM-28), solid black circles; sector-zoned garnet from a pelitic schist (PCM-618) in contact with a quartz vein, solid black stars; sector-zoned garnet from a diopside-bearing calc-silicate rock (RCS-2), solid grey stars.

7.175. The Mg/(Mg+Fe^{2+}) ratio ranges from 0.58 to 0.88. Al^{IV} and Al^{VI} in amphibole are 0.825-1.970 and 0.267-0.910, respectively. Plotted data are mainly found in the boundary between tschermakite and Fe-tschermakite, and the amphibole analyzed in this study is Fe-hornblende. The Si^{IV} ranges from 5.890-7.017. The Mg/(Mg+Fe^{2+}) ratio ranges from 0.43-0.95. Figure 10 b shows as the substitution of Al^{IV} tetrahedral sites is coupled with that of Al^{VI} in octahedral sites. Al^{IV} and Al^{VI} in amphibole are 1.159-1.811 and 0.299-0.985, respectively.

Scapolite representative analyses are given in Table 3. The chemical composition of scapolite, according to the EqAn = 48.47%, corresponds to meionite (a calcium-rich mineral), one of the three end-members that define the scapolite solid solution. The sum of Ca + Na + K is 4.42 pfu.

Other minerals. Representative analyses of other minerals are given in Tables 2-4. The anorthite content (X_{An}) of plagioclase is variable in both metacarbonate and related rocks (0.03 to 0.99). In pelitic schists this content varies from 0.30 to 0.34. An increase in X_{An} of plagioclase rims in contact with garnet appears to be related to the depletion of X_{grs} of garnet rims in pelitic rocks, whereas in metacarbonate or associated rocks such increase should be related to plagioclase rims in contact with amphibole. The mineral phases of the epidote-group contain minor amounts of Mn (0.000-0.021). The Fe^{3+}/(Fe^{3+}+Al) ratio ranges from 0.08-0.26. The analyzed grains probable correspond to clinozoisite, which is rich in Fe^{3+}, but in general it ranges between 0.355 and 1.629 pfu, and individual samples show significant chemical variations. It shows commonly optical zoning, but its chemical zoning patterns often show inconsistent relationships. Biotite is in the compositional range reported by García *et al.* (2005), with TiO_2 content between 0.93 and 3.31, X_{Mg} = 0.21-0.76, Al^{IV} = 2.273-2.833 and Al^{VI} = 0.552-0.913, indicating slight solid solution towards dioctahedral micas. Si content of muscovite ranges from 6.211 to 6.492. The celadonite content, (Si/2)-3, varies from 0.11 to 0.12 and the Na/(Na+K) ratio from 0.00 to 0.12, which are in the compositional range reported by García *et al.* (2005). According to the classification proposed by Hey (1954), chlorite ranges in composition from pycnochlorite to brunsvigite. Chlorite is Mg-rich chlorite (X_{Mg} = 0.46-0.71) and contains small amounts of Mn, which ranges from 0.000 to 0.077. Al_2O_3 (2.76 wt%) and Fe_2O_3 (0.60 wt%) contents of titanite are low in the analyzed sample, and X_{Al} = 0.10. Calcite is almost pure $CaCO_3$. Only samples whose Ca fraction was greater than 0.85 were used in the calcite-dolomite thermometry.

Physical conditions during metamorphism

Metamorphism in the CSM occurred under conditions of high-temperature and medium-pressure (Barrovian type metamorphism), and reflects the high heat flow that exists in this part of the Santander Massif. Additional constraints in our calculations are given by the P-T conditions deduced by Castellanos (2001) and García *et al.* (2005) for the metapelitic sequence exposed in this region. According to their geothermobarometry results, the pressure and temperature conditions in the staurolite-kyanite zone are in the range of 6.2-7.4 kbar and 616-698°C, respectively. Temperatures from the Mg content in calcite coexisting with dolomite have been determined using the equation of Rice (1977):

$$T(K)^{-1} = \frac{\ln X_{MgCO_3}^{Cc}}{-3\cdot 8\times 10^{3}} + 4\cdot 704\times 10^{-4}.$$

This calibration is based on a least squares fit to the experimentally determined solvus at 2 kbar (Graf & Goldsmith, 1955; Goldsmith & Newton, 1969). The temperature obtained in the Silgará Formation ranges between 286 and 377°C, which can be attributed to a retrograde metamorphism. However, using the thermometer of Goldsmith & Newton (1969) we obtained a range in temperature of 470-550°C as illustrated in Figure 11, which corresponds to the diagram of calcite–dolomite thermometry of Anovitz & Essene (1987) also used by Piazolo & Markl (1999) to place lower boundary constraints on the metamor-

Table 4. Representative analyses and chemical formulas of the minerals in a calc-silicate rock (sample RCS-2) of the Silgará Formation.

Mineral	Grt	Grt	Fe-Ts	Mg-Hbl	Fe-TS	Pl	Pl	Pl	Kfs	Czo	Zo	Ttn	Cal	Chl	Sep
Analysis	1 (core)	2 (rim)	18	19	27	30	14	15	21	3	24	9	6	10	8
SiO_2	37,34	38,05	53,38	52,53	46,89	47,30	60,12	63,53	64,95	38,46	40,77	31,83	0,00	0,00	0,00
TiO_2	0,00	0,00	0,00	0,37	0,28	0,39	0,00	0,00	0,35	0,38	0,00	36,43	0,00	0,00	0,00
Al_2O_3	21,03	20,86	0,92	1,44	8,84	9,98	22,69	21,68	18,98	29,39	27,34	2,76	0,00	20,43	24,59
FeO	26,79	18,50	11,40	12,12	19,94	18,99	0,00	0,00	0,00	4,87	3036,00	0,60	0,51	23,10	0,58
MnO	5,39	4,27	0,45	0,44	0,38	0,45	0,00	0,00	0,00	0,00	0,00	0,00	0,35	0,44	0,00
MgO	1,69	1,07	10,70	10,51	8,29	8,25	0,00	0,00	0,00	0,00	1,61	0,00	0,26	16,14	0,00
CaO	7,43	16,19	23,43	22,68	11,89	11,61	7,22	4,69	0,79	23,72	22,81	29,17	53,35	0,18	26,85
Na_2O	0,31	0,37	0,49	0,49	0,69	0,92	9,64	9,13	0,53	0,28	0,30	0,00	0,27	0,37	0,00
K_2O	0,00	0,00	0,00	0,00	0,34	0,21	0,00	0,18	14,87	0,00	0,00	0,00	0,00	0,00	0,00
Total	100,38	99,33	100,77	100,58	97,54	98,10	99,67	99,21	100,47	97,10	96,19	100,79	54,74	88,56	96,99
Oxygen basis	12	12	6	6	23	23	8	8	8	25	25	5	3	28	25
Si	3,017	3,023	2,004	1,981	7,017	6,994	2,711	2,833	2,972	6,04	6,378	1,02615	0	5,735	6,912
Ti	0,000	0,000	0,000	0,010	0,032	0,043	0,000	0,000	0,012	0,045	0,000	0,883	0,000	0,000	0,000
Al	1,981	1,953	0,041	0,064	1,559	1,739	1,206	1,140	1,024	5,439	5,040	0,105	0,000	4,949	4,454
Fe^{3+}	0,000	0,000	0,000	0,000	0,267	0,204	0,000	0,000	0,000	0,639	0,440	0,016	0,000	0,000	0,000
Fe^{2+}	1,791	1,229	0,358	0,382	2,243	2,155	0,000	0,000	0,000	0,000	0,000	0,000	0,0220	3,970	0,075
Mn	0,365	0,287	0,014	0,014	0,048	0,056	0,000	0,000	0,000	0,000	0,000	0,000	0,015	0,077	0,000
Mg	0,021	0,129	0,599	0,591	1,849	1,819	0,000	0,000	0,000	0,000	0,375	0,000	0,020	4,946	0,000
Ca	0,636	1,378	0,942	0,916	1,906	1,839	0,349	0,224	0,039	3,991	3,823	1,007	2,930	0,040	4,421
Na	0,100	0,118	0,036	0,036	0,200	0,264	0,843	0,789	0,047	0,085	0,091	0,000	0,027	0,147	0,000
K	0,000	0,000	0,000	0,000	0,065	0,040	0,000	0,010	0,868	0,000	0,000	0,000	0,000	0,000	0,000
Total	8,092	8,119	3,993	3,994	15,186	15,153	5,108	4,997	4,961	16,239	16,147	3,038	3,013	19,864	15,861
X_{Mg}	0,1	0,1	0,63	0,61	0,45	0,46								0,55	0,00
X_{An}							0,43	0,34							
X_{Al}												0,10			
Al_2Fe %										15,68	12,63				
EqAn															48,47

* X_{Al}= Al/(Al+Ti+Fe^{3+}); Al2Fe%=Fetot/(Fetot+Al-2)*100;EqAn=(Al-3)/3*100

phic temperature conditions experienced by the marbles. According to these authors, a temperature of 625°C should be interpreted as the minimum reequilibration temperature at amphibolite facies conditions. A range of temperature data reported by them shows equilibration at still lower temperatures of approximately 500°C, which is similar to the temperatures estimated in this study. Since the Mg content of the calcite is commonly reduced by retrograde exsolution of dolomite and/or recrystallization, temperature estimates based on the calcite–dolomite solvus often represent a minimum temperature of for-

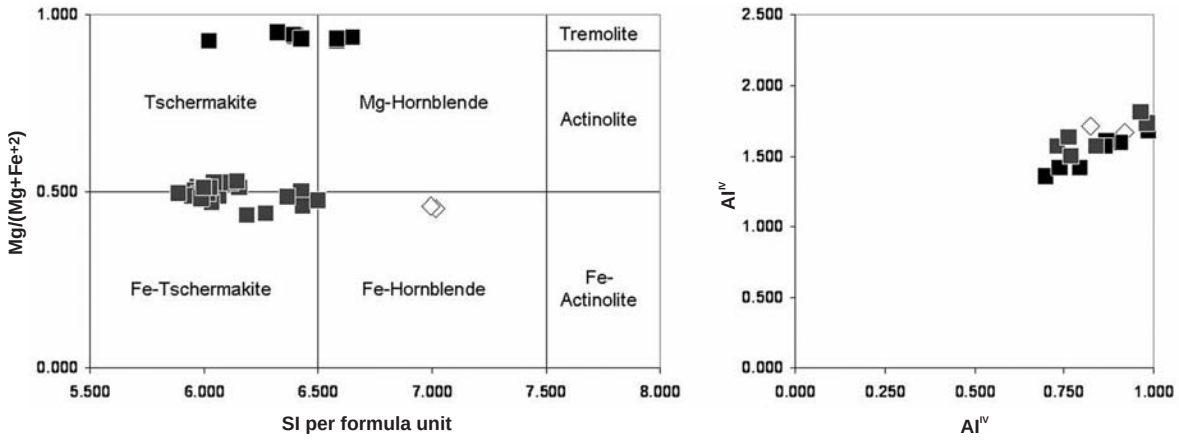

Figure 10. Chemical composition of amphibole in metacarbonate and related rocks of the Silgará Formation. Left side, based on 23 oxygen per formula unit (pfu) (after Leake, 1978). CaB=1.5; (Na+K)A<0.5; CaA<0.5. Right side, expressed by the ALIV vs. ALVI variation. Symbols correspond to garnet-bearing amphibolite (PCM-128), solid black squares; garnet-bearing amphibolite in contact with pelitic schist (PCM-28), solid grey squares; diopside-bearing calc-silicate rock (RCS-2), open black rhombs.

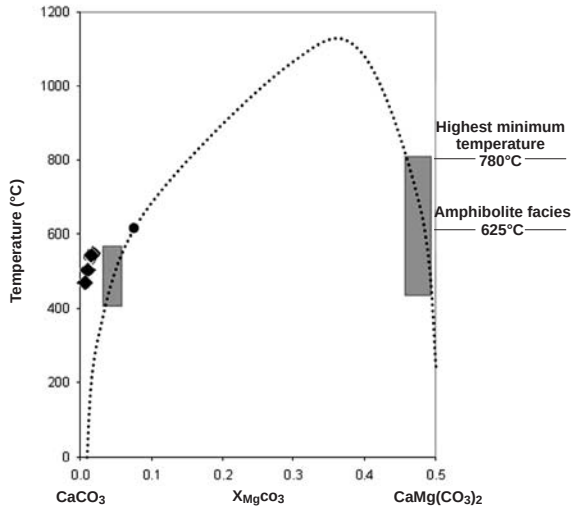

Figure 11. Diagram of calcite–dolomite thermometry modified after Anovitz & Essene (1987); the grey areas represent the range of temperature obtained by Piazolo & Markl (1999), and the black dot indicates a reintegrated sample yields a temperature of 625°C. Temperatures obtained in this study after Goldsmith & Newton (1969) are indicated by black rhombs; T = 3O8O/[(-lnX_{MgCO3})+ 1.54], when 0.04 < X_{MgCO3} < 0-14.

mation (Essene, 1983). Furthermore, in the absence of dolomite, the calcite compositions can only be used to estimate minimum temperatures. The Silgará Formation was affected by a regional metasomatism, and the mineral phases present in the metasomatic zones are consistent with a high activity of CO_2 (relative to H_2O) in the grain-boundary phase during prograde metamorphism, and a high activity of H_2O during retrograde metamorphism. However, additional work is needed to determine the nature of the metasomatic reactions, although it is probably that elements, such as Fe, K, Al, Ti and Si were introduced to the chemical system to produce calcite, potassium feldspar, Fe-Mg silicates, scapolite, and titanite. These elements, although their source is unknown, presumably entered the rocks by way of a grain-boundary phase evidently rich in H_2O relative to CO_2, causing graphite to disappear, as discussed by French (1966). The common components in these rocks include Mg, Mn and Fe^{3+} (in garnet), Mg and Fe^{3+} (in clinopyroxene), Na (in scapolite and plagioclase) and H_2O (in the vapor phase). Effects of these additional components have a marked influence on the stability fields of the garnet-bearing and garnet-absent assemblages. At lower temperature

(<600°C), introduction of H_2O in the system will stabilize hydrous phases, such as amphibole or epidote-group minerals. Na enters the structure of plagioclase and scapolite. As a consequence with the entry of Na_2O in the system, the fields of scapolite-bearing assemblages will expand at the expense of garnet-bearing assemblages. The introduction of Mg and Mn to the system does not introduce any new phase, although these elements are strongly partitioned in the structures of clinopyroxene and garnet. Mn in addition enters the structure of calcite to some extent. Our results will be briefly compared with those obtained from Castellanos (2001) and García *et al.* (2005) in the metapelitic sequence of the Silgará Formation at the CSM, where this geological unit consists dominantly of greenschist to amphibolite facies rocks.

Phase relationships

The metacarbonate and related rocks of the study area are very complex metamorphic rocks in which various chemical reactions have taken place to produce the minerals assemblages that are presently found within them. The above information on the association of minerals and their chemical composition will now be used in combination with experimental data, where available, to determine as far as possible the nature of the chemical reactions that have taken place and the conditions of pressure and temperature of metamorphism. The mineralogy of the metasomatic rocks of the Silgará Formation can be examined in the CaO-Al_2O_3-FeO-MgO-K_2O-Na_2O-MnO-Fe_2O_3-TiO_2-H_2O-CO_2 chemical system, in the presence of SiO_2 (quartz) and a H_2O-CO_2 binary fluid. Lopez & Soto (1999) have deduced from an ACF diagram (Figure 12a) that the formation of the mineral assemblages in calc-silicate rocks is due to an increase in the chemical potential (μ) of CaO from pelitic rocks to marble, which is balanced by diffusion of Al_2O_3 (and probably SiO_2) in the opposite direction. These authors consider that the occurrence of quartz in all the reported zones indicates that μSiO_2 remained constant during this process. The mineralogy and the compositional variation of minerals from a representative calc-silicate rock of the Silgará Formation, containing the defined reaction zones, are depicted in an ACF projection (Figure 12b). T-X_{CO2} diagrams are used to predict the sequence of metamorphic mineral assemblages that would be ob-

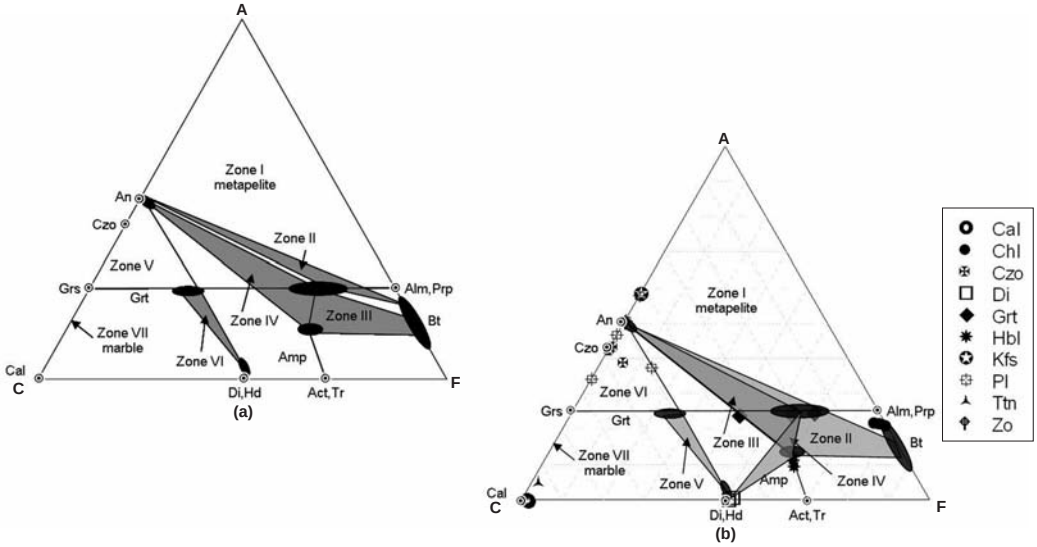

Figure 12. (a) ACF diagram with the mineral assemblages from different reaction zones (light gray fields) found in a calc-silicate rock by Lopez & Soto (1999). Dark gray fields represent chemical analyses of minerals from reaction zones. A = Al2O3 + Fe2O3; C = CaO; F = FeO + MgO. (b) ACF projection showing the mineralogy and compositional variation of minerals from a representative calc-silicate rock of the Silgará Formation at CSM

served at constant fluid composition as shown in Figure 13. However, this metamorphism, although easy to understand, is probably not representative of natural processes. The reactions encountered in progressive metamorphism generate H_2O and CO_2 that will tend to change the fluid composition, and representing a problem. A process that serves very well to drive devolatization reactions is infiltration by fluids (Spear, 1993). Changing fluid composition at constant temperature and pressure is just as effective for driving reactions as changing the temperature or pressure at constant fluid composition. Numerous mineral reactions should take place in the investigated rocks during metamorphism. The calcite-dolomite reaction, which controls the Mg content of calcite, indicates retrograde metamorphic temperatures of 470-550°C. The Mg content of calcite in equilibrium with dolomite was shown by Harker & Tuttle (1955), Goldsmith & Heard (1961) and Goldsmith & Newton (1969) to increase with rising temperature. However, some obstacles that are normally encountered in carrying out an interpretation of mineral assemblages in these petrochemical type of rocks are: (1) generally it is not yet possible to identify using textural features of the rock, the reactants that produced a mineral presently found; (2) the primary or secondary nature of dolomite and quartz in some of rocks is unclear; (3) in rocks undergoing metamorphism, a gaseous phase may not be present and molecules of H_2O and CO_2, as well as other relatively volatile constituents, may be concentrated in a grain-boundary phase (Ramberg, 1952; Thompson, 1955; Barth, 1962); (4) normally, in dealing with natural mineral assemblages, the minerals are not "pure" and one or more compositional variables must be considered in addition to variation in the concentration or activity of H_2O and CO_2.

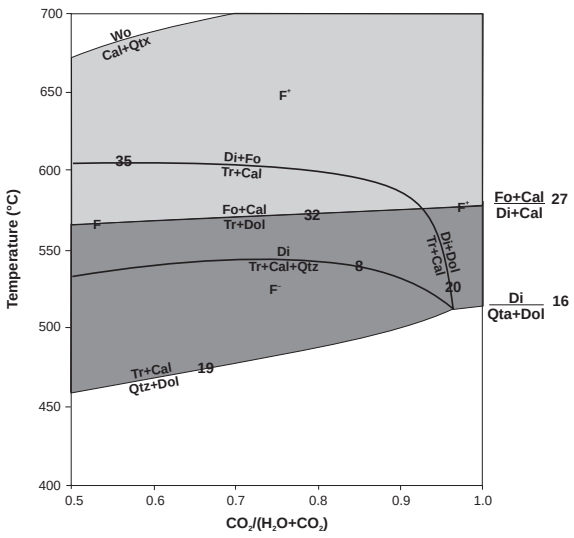

Figure 13. T-X($_{CO2}$) diagram, showing boundary curves for carbonate-silicate reactions, according to Skippen (1971); total pressure is 2 kbar. The wollastonite curve at top-left is from Greenwood (1967). F-, F and F+ symbolize the forsterite-forming reaction not initiated, in progress, and completed (Kretz, 1980).

Quartz and dolomite are considered to be incompatible, whereas quartz and calcite are commonly found in contact, without sign of reaction to produce wollastonite. Therefore, since quartz and dolomite are considered to have been incompatible everywhere in the field area and wollastonite was not found in quartz-calcite rocks, the area of interest in relation to Figure 13 lies between the line defined by reactions 19 and 16 at low temperatures and the wollastonite curve at high temperatures. However, this area is divided into two sub-areas, designated F^- and F^+, separated by the two forsterite-forming curves, 32 and 27, labeled F. In this study however this area should be reduced up to the reaction 27, because until now there is not evidence of the occurrence of forsterite in metacarbonate and related rocks. Several possibilities would exist concerning the nature of the reactions that have produced amphibole, pyroxene and scapolite during metamorphism. Amphibole that approximates tremolite in composition probably formed from quartz and dolomite (reaction 19), although amphibole contains appreciable Al, Na, and K, these elements may have been derived from detrital plagioclase and muscovite (Kretz, 1980). Reaction rims of amphibole around pyroxene, and where this reaction has finished, amphibole apparently formed after pyroxene according to reaction 20 (no quartz inclusions are present) or 8 (quartz inclusions are present). Chemical reactions de-

scribed above can take place in response to an increase in the activity of H_2O relative to that of CO_2 or to a decrease in temperature. Diopside has probably formed from amphibole via reactions 8 or 20, in which small amounts of Al, Na, K, and Fe can be derived from amphibole and, alternatively, it can be formed directly from dolomite by reaction 16, which appears to be responsible for the occurrence of pyroxene-rich assemblages.

On the other hand, the presence of titanite is of interest in relation to the reaction:

rutile + calcite + quartz = titanite + CO_2,

which was investigated by Hunt & Kerrick (1977), who located the reaction at 500°C for a total pressure of 2 kbar and an intermediate CO_2:H_2O ratio. The examined metasomatic rocks evidently reached higher temperatures, titanite should be present in place of rutile and quartz, as found. Titanite is particularly common and abundant in these rocks, and it was probably formed by metasomatic introduction of titanium. The rare presence of grossularite is of interest in relation to the experiments and calculations of Gordon & Greenwood (1971), who showed that at 600-700°C and 2 kbar this mineral is stable only in the presence of H_2O-rich fluids, with $CO_2/(H_2O + CO_2) < 0$-2. Under these conditions of pressure and fluid composition and at a temperature less than about 600 °C, grossularite may crystallize according to the reaction:

calcite + anorthite + quartz = grossularite + CO_2.

No information is available concerning the reaction by which scapolite crystallized in these rocks. Scapolite is apparently the product of metasomatism, which implies an introduction of various elements, including Cl and S, possibly as Cl_2 and SO_2 (Kretz, 1980). Most of the retrograde reactions, including the exsolution of calcite, are considered to have taken place during a cooling process, following the thermal climax, and no attempt will be made to estimate the temperature of these reactions. All reactions, particularly those that require H_2O can take place below the equilibrium temperature, so that a condition of near-equilibrium between reactants and products was never attained. The distribution of minor elements between associated calcite and dolomite may be examined in relation to chemical exchange reactions and the concept of exchange equilibrium. These reactions, although they do not produce new mineral phases, represent one of the several different kinds of chemical changes that take place in metamorphic rocks, all of which are expected to proceed toward equilibrium and a minimum of free energy.

The application of the phase rule to these chemical open systems and the determination of the stability conditions of the mineral assemblages assume local equilibrium (Thompson, 1959). Fluid flow plays a very important role in heat and mass transfer in the crust and is strongly controlled by the layered permeability structure (Cui *et al.*, 2001). Calc-silicate rocks represent only a small fraction of the crust, but they are valuable monitors of fluid flow and fluid-rock interaction and can reveal significant information about the composition of the metamorphic fluid phase and P-T conditions (Ague, 2003). The regional fluid flow transporting volatiles including H_2O and CO_2 is an integral part of prograde regional metamorphism. According to Ague (2003), metacarbonate rocks are commonly out of chemical equilibrium, at least in part, with surrounding lithologies such as metaclastic rocks, and consequently, fluids that infiltrate metacarbonate layers can drive significant chemical reaction involving volatiles and other elements, particularly at lithologic contacts (e.g., Ague, 2000) and in alteration zones or "selvages" around syn-metamorphic veins (e.g., Ague & Rye, 1999; Ague, 2002). It is probably that mass transfer of "non-volatile" rock-forming elements has been significant during regional metamorphism of metacarbonate rocks in the Silgará Formation at the CSM, taking into account that evidence of this has been reported in similar geological contexts around the world (e.g., Thompson, 1975; Brady, 1977; Tanner & Miller, 1980; Tracy *et al.*, 1983; Leger & Ferry, 1993; Ferry, 1994; Ague & van Haren, 1996; Widmer & Thompson, 2001; Shmulovich *et al.*, 2001; Carlson, 2002). We con-

sider that H_2O required to drive prograde CO_2 loss probably came from regional dehydration of surrounding metapelitic schists, although the development of a H_2O-rich diopside reaction zone in the presence or absence of scapolite probably also required an external fluid contribution derived from syn-metamorphic intrusions (orthogneiss masses) emplaced during the final stage of metamorphism of the Silgará Formation.

Discussion (origin of the reaction zones)

Devolatilization of metasedimentary sequences is a process occurs during regional metamorphism and play a very important role in the cycling of volatiles through the that Earth's, and metacarbonate rocks are the source of most of the CO_2 evolved by regional metamorphism, although considerable uncertainly remains regarding the process of fluid release and transport (Ague, 2002). Devolatilization presumably resulted from heating and fluid flow during dynamic regional metamorphism of the Silgará Formation, and that the calc-silicate reaction zones occurring in metacarbonate and related rocks of this metamorphic unit contain mineral assemblages representing the greatest amount of devolatilization reaction progress, which has been documented by Hewitt (1973) at the edges of the metacabonate layers in contact with surrounding pelitic schists and in reaction selvages adjacent to syn-metamorphic quartz veins. Many of the studied calc-silicate rocks, especially in the case of the diopside-bearing type rocks, appear as clearly defined reaction zones with a mineral composition that evolves from pelitic schists to marbles or carbonate-silicate rocks. This sequence of zones is similar to those described in other calc-silicate reaction zones (e.g., Thompson, 1975; Kerrick, 1977; Ague, 2002, 2003).

Ague (2003) estimated fluid compositions in metacarbonate rocks, giving particular attention to the reaction diopside-rich zones, which show the higher H_2O-rich compositions, as required by the topology of the diopside-producing reactions. Hewitt (1973) inferred a large gradient in fluid composition across a lithologic contact based on a sharp in anorthite content of plagioclase from metacarbonate to metapelitic layers, which necessarily not indicate change in X_{CO2}, taking into account that the mineral assemblages in the two layers are very different. On the other hand, Tracy *et al.* (1983) inferred large changes in X_{CO2} across a reaction zone adjacent to quartz veins.

According to Ague (2002), the mineral assemblages of the diopside-rich zones are stable at high T (> c.575ºC) and relatively low X_{CO2}. This author also consider that the low X_{CO2} fluid of the diopside-rich zones was present at peak P-T conditions that can not be differentiated from those of the immediately adjacent zones, implying that pressure and temperature were not the main variables controlling their formation. It is probable that prograde reactions and CO_2 loss have occurred in the metacarbonate layers within the Silgará metamorphic sequence in response to (1) infiltration of H_2O from dehydration of surrounding pelitic schists (e.g., Hewitt, 1973; Ague & Rye, 1999; Ague, 2000) or (2) advection-driven infiltration of a H_2O-rich fluid external to the metasedimentary sequence (e.g., Tracy *et al.*, 1983; Ague & Rye, 1999; Ague, 2002). Therefore, we adopted the model of Ague (2003) to explain the origin of the reaction zones observed within metacarbonate and related rocks of the Silgará Formation at CSM, considering a fluid flow (advection) in metacarbonate layers parallel to the lithological boundaries and a transport (diffusion and dispersion) occurring across the layers as illustrated in Figure 14. In this model, CO_2 produced is transported across the layers by hydrodynamic dispersion, but also it can be transported by advection following parallel to the layers.

Therefore, it is probable that a low X_{CO2} of the reaction zones investigated in this work was produced when the fluid produced by the dehydration of surrounding Silgará pelitic schists combined with an external H_2O-rich fluid, which evolved from syn-metamorphic magmas (orthogneiss masses) that were emplaced at the lowest structural levels of the Silgará Formation, penetrating mainly along contacts and through fractures.

The presence of clinozoisite in the calc-silicate rocks suggests an extremely low X_{CO2} as been pro-

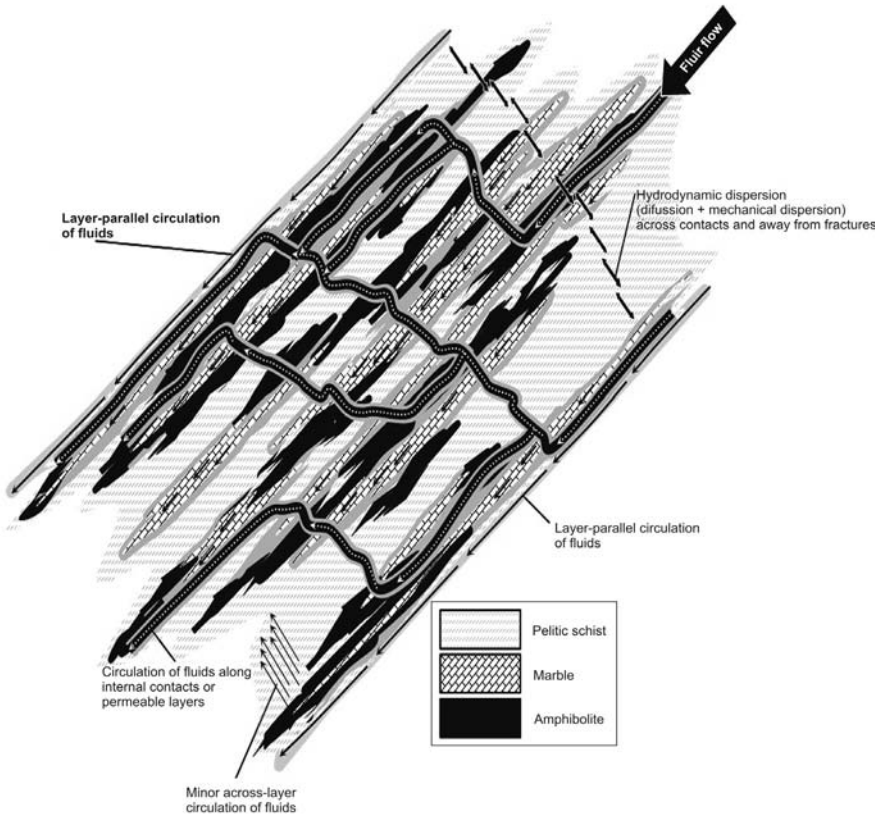

Figure 14. Schematic cross-section of metacarbonate layers illustrating infiltration processes, in which the circulation of fluids is mostly layer-parallel or through fractures. Observe the circulation of fluids concentrated along lithologic contacts and through fractures and permeable layers. Hydrodynamic dispersion (diffusion and mechanical dispersion) occurred at high angles to circulation of fluids. Largest amounts of fluid-rock reaction and metasomatism denoted by dark gray shading; lesser amounts by lighter gray shading. Metasomatic effects envisioned to have propagated into the metacarbonate layer: inward from its margins and away from fractures or permeable horizons. Adapted and modified after Ague (2003).

posed in other studies (e.g., Thompson, 1971; Storre & Nitsch, 1972).

These reaction zones are characterized by sharp contacts and a low number of phases that are stable in each zone and their formation could be controlled by diffusion processes as been proposed in other studies (e.g., Thopmson, 1975; Joesten, 1977, 1991; Ague & Rye, 1999; Ague, 2000, 2002, 2003). Another possible origin for the reaction zones, suggested for other calc-silicate rocks, could be an infiltration process. For the calc-silicate rocks examined in this work, some arguments suggest a limited influence of this factor: (1) metamorphic rocks have low porosity (Brady, 1977), fluid circulation would be restricted, producing small-scale reaction bands; (2) infiltration processes generate an asymmetric distribution of calc-silicate bands from metapelites to marbles or carbonate-silicate rocks on both sides of the metapelite intercalations (Lopez & Soto, 1999). A strong evidence for a limited infiltration of aqueous fluids is observed in the diopside-rich zones with the consumption of graphite and the production of scapolite (Nabelek, 2002). Therefore, an infiltration process should be consider in the development of these calc-silicate rocks, which can be reviewed to estimate if it would produce a larger variation in the chemical composition of the minerals compared with the data presented here.

The investigated calc-silicate rocks can be developed as a result of an isochemical metamorphism of pure carbonate rocks (e.g., marbles) or by metasomatic introduction of silica into them or by a combination of these processes. On the other hand, marble layers recognized in the metamorphic sequence of the Silgará Formation at CSM have not enough silica to produce the calc-silicate rocks, in spite of metacarbonate and related rocks with some silica content and quartzites also occurs. According to Campos (1999), the occurrence of veins mainly composed of quartz with minor calcite in the metasomatic zones indicates that a remobilization of SiO_2 and CaO can be due to the action of late magmatic fluids associated to the emplacement of the Orthogneiss protolith, which circulated along tectonic discontinuities or schistosity surfaces. We adopt the term "barren calc-silicate rocks" to metacarbonate and related rocks occurring at this region, taking into account that they are characterized by the presence of diopside and scapolite, although lacking wollastonite. We can differentiate these rocks from wollastonite-bearing calc-silicate rocks which are produced by metasomatism of almost pure carbonate rocks. Circulating fluids would react with the carbonates and convert them to calc-silicates, and when all carbonate was used up there would be no more reactions, and the silica would be transported elsewhere, as it is soluble in hydrothermal fluids. Therefore, the absence of wollastonite-bearing calc-silicate rocks at the CSM can be explained by the fact that these rocks require either a protolith richer in calcite than the barren calc-silicate rocks or loss of Mg during metasomatism. However, if the calc-silicates were produced by metasomatism, additional chemical effects of this process should be explained.

The fluid flow plays a very important role in heat and mass transport in the crust and is strongly controlled by the layered permeability structure, which causes focused subhorizontal fluid flow within high permeability lithologic units Cui *et al.*, 2001). Although a component of fluid flow was subhorizontal along bedding, a larger component must have been subvertical through fractures that cut across the calcareous layers (e.g., Cui *et al.*, 2001; Nabelek, 2002). The effects of transient permeability changes associated with mineral reactions on heat and fluid flow, which are very important for layered metasedimentary sequences where metamorphic devolatilization reactions are likely to be more extensive in calc-silicate layers than in either limestone or shale layers, are not well understood (e.g., Hover-Granath *et al.*, 1983). These authors determined that metamorphic reactions in marble layers occur in equilibrium with a CO_2-rich fluid phase at all grades, while in calcareous argillite layers they occur in the presence of progressively more H_2O-rich fluids as metamorphic grade increases.

According to Ague (2003), the increases in metasomatic mass transfer toward contacts and veins demonstrate the importance of hydrodynamic dispersion along gradients in fluid composition at high angles to layering and in alteration selvages, consistent with the results of reaction-transport modeling. The regular sequences of mineral assemblages observed at lithologic contacts and in vein selvages, which have not yet established at the CSM, are classic indicators of hydrodynamic-dispersion mass transfer (e.g., Vidale, 1969; Hewitt, 1973; Vidale & Hewitt, 1973; Thompson, 1975; Brady 1977; Ashworth & Sheplev, 1997; Abart *et al.*, 2001, Ague, 2003).

The reaction-transport modeling indicates limited cross-layer advection (Ague, 2003), so most of the regional fluid flow presumably occurred parallel to layering or through fractures (Figure 14), which is consistent with previous studies carried out in other metamorphic belts (e.g., Hewitt, 1973; Rye *et al.*, 1976; Tracy *et al.*, 1983; Bickle & Baker, 1990; Ague, 1994; Ferry, 1994; Ague, 2000, 2003). A considerable component of the layer-parallel flow was concentrated along metapelitic-metacarbonate contacts and internal contacts separating reaction zones with differing properties (such as grain size and mineralogy) within individual metacarbonate layers, which is supported by local source-sink relationships and fractures (Ague, 2003). Metacarbonate and metapelitic rocks have different physical properties, so contacts between them are favorable areas of mechanical weakness, in some cases related to elevated fluid pressures during reaction (Walther, 1996).

Fracturing at lithologic contacts increased porosity and permeability (Ague, 1995); so highly veined contacts were probably sites of elevated fluid flux relative to more "pervasive" flow through non-fractured rock matrix (Breeding *et al.*, 2003). In addition, reactions driven by fluids infiltrating along contacts may have increased rock porosity and permeability at the grain scale and focused layer-parallel flow into the contact areas (Balashov and Yardley, 1998). Most veins that cross-cut metacarbonate layers are surrounded by reaction selvages whose mineral assemblage zonation is similar to that found at lithologic contacts. Advective fluid flow transported the chemical "signature" of the surrounding rock types into the metacarbonate layers along the cracks and in the immediately adjacent wall rock. Hydrodynamic dispersion at high angles to the crack walls operated to transport mass to and from fractures and form the altered selvages. Next to some veins, quartz, calcite, feldspar, titanite, and/or rutile were removed from the wall rock and deposited in the adjacent vein. This local transport or "segregation" is inferred to have occurred by processes dominated by diffusion (e.g., Ague, 2003), and did not necessarily require large fluid fluxes.

Concluding Remarks

A large volume of studies exists on the metamorphism of calc-silicate rocks. However, one of the main reasons for studying these rocks is due to the mineral assemblages are a function of the composition of the fluid, studying the distribution of the mineral assemblages provide considerable information about the behavior of the fluid phase during metamorphism. During the development of the calc-silicate reaction zones between marble and pelite layers, a volume of these lithologies should have disappeared. Garnet-bearing rocks display a sequence of textural and compositional zones with different high-variance mineral assemblages, which can be interpreted as a consequence of diffusion processes (mainly transfer of CaO) between adjacent impure calcite-bearing marble and aluminum-rich metapelites.

The mineral assemblages up to the appearance of scapolite in the diopside-rich zone give little evidence about the compositions of fluids that existed in the rocks during metamorphism, except that if there was very little or an absence of fluid infiltration, the reactions would have driven $X(_{CO2})_{fluid}$ to higher values (Nabelek, 2002). The first direct evidence for infiltration of aqueous fluids occurs in the diopside-rich zone with the consumption of graphite and the production of scapolite.

There is not doubt that marble has decomposed releasing CO_2 from the chemical system and CaO to the pelite. Although compositional gradients in the CO_2-H_2O-fluid produced by decarbonation of marble and dehydration of pelite should be considered, it is probably that the amount of circulation of fluids may not have been important. However, it is difficult to establish if the cation diffusion process dominates respect to the fluid flow as the mechanism of mass transfer as been proposed by Thompson (1975), taking into account that in the Silgará Formation metamorphic rocks the circulation of fluids through fractures and lithologic contacts has played a very important role in the development of hydrothermal veins, some of which are observed within calc-silicate reaction bands. Therefore, future research should consider in detail the geometry of the calc-silicate reaction zones to distinguish between diffusion and flow fluid processes, which require more information on the properties of aqueous fluids, mineral phase stability and chemical compositions of coexisting phases in the mineral assemblages in order to develop a model for a metasomatic phenomenon.

These metamorphic conditions agree well with those estimated by Garcia *et al.* (2005) for the high-grade metapelites of the Silgará Formation at the CSM in which are intercalated the metacarbonate and related rocks and also with the P-T conditions deduced for metapelites. This research has shown that phase-relationship analysis of reaction zones developed along metapelite-marble contacts represent a powerful tool contributing to understanding the metamorphic evolution of the Santander Massif in the geological context of the Colombian Andes.

We propose the name of a non economic mineralization "reaction calcic exoskarn" (except by the exploitation of marble) for the metacarbonate and related rocks that form part of the metamorphic sequence of the Silgará Formation at the CSM, taking into account the composition and texture of the resulting skarn, the available terminology for these rocks, and the following aspects suggested by Meinert (1992): (1) skarns can form during regional or contact metamorphism and from a variety of metasomatic processes involving fluids of different origin (magmatic, metamorphic, meteoric, and/or marine); (2) they can be found adjacent to plutons, along faults and major shear zones, in shallow geothermal systems, on the bottom of the seafloor, and at lower crustal depths in deeply buried metamorphic terrains; (3) what links these diverse environments, and what defines a rock as skarn, is the mineralogy, which includes a wide variety of calc-silicate and associated minerals but usually is dominated by the presence of garnet and diopside. The "reaction calcic exoskarn" that crops out at the CSM probably has developed by isochemical metamorphism of thin interlayered shale and carbonate levels where metasomatic transfer of components between adjacent lithologies (e.g., Zarayskiy *et al*., 1987) may occur on a millimeter to centimeter scale. It is known that the composition and texture of the protolith tend to control the composition and texture of the resulting skarn. On the other hand, most economically important skarn deposits (which are not our case) result from large-scale metasomatic transfer, where fluid composition controls the resulting skarn and ore mineralogy.

Acknowledgements

The present work forms part of the undergraduate Thesis carried out by S. Gómez and G. Avila at Universidad Industrial de Santander. We are very grateful to the Universidad Industrial de Santander, entity that supported fieldwork. We are indebted to doctors Alan Boyle from the Department of Earth & Ocean Sciences at University of Liverpool (England) and Akira Takasu from the Department of Geosciences at Shimane University (Japan) for contributing us with the acquisition of electron backscatter diffraction and electron microprobe analyses. The authors also acknowledge to the anonymous referees for their critical and insightful reading of the manuscript. We are most grateful to the above-named people and institutions for support.

References

Abart, R., Schmud, R., and Harlov, D. (2001). Metasomatic coronas around hornblendite xenoliths in granulite facies marble, Ivrea zone, N Italy I: Constraints on component mobility. Contributions to Mineralogy and Petrology, Vol. 141, pp 473-493.

Ague, J. (1994). Mass transfer during Barrovian metamorphism of pelites, south-central Connecticut. II: Channelized fluid flow and the growth of staurolite and kyanite. American Journal of Science, Vol. 294, pp. 1061-1134.

Ague, J. (1995). Depth crustal growth of quartz, kyanite, and garnet into large aperture, fluid-filled fractures, north-eastern Connecticut, USA. Journal of Metamorphic Geology, Vol. 13, pp. 299-314.

Ague, J. (2000). Release of CO_2 from carbonate rocks during regional metamorphism of lithologically heterogeneous crust. Geology, Vol. 28, pp. 1123-1126.

Ague, J. (2002). Gradients in fluid composition across metacarbonate layers of the Wepawaug Schist, Connecticut, USA. Contributions to Mineralogy and Petrology, Vol. 143, pp. 38-55.

Ague, J. (2003). Fluid infiltration and transport of major, minor, and trace elements during regional metamorphism of carbonate rocks, Wepawaug Schist, Connecticut, USA. American Journal of Science, Vol. 303, pp. 753-816.

Ague, J., and Rye, D. (1999). Simple models of CO_2 release from metacarbonates with implications

for interpretation of directions and magnitudes of fluid flow in the deep crust. Journal of Petrology, Vol. 40, pp. 1443-1462.

Ague, J., and van Haren, J. (1996). Assessing metasomatic mass and volume changes using the bootstrap, with application to deep-crustal hydrothermal alteration of marble. Economic Geology, Vol. 91, pp. 1169-1182.

Anovitz, L., and Essene, E. (1987). "Equilibria in $CaCO_3$-$MgCO_3$-$FeCO_3$." Journal of Petrology, Vol. 28(2). pp 389-414.

Ashworth, J., and Sheplev, V. (1997). Diffusion modeling of metamorphic layered coronas with stability criterion and consideration of affinity. Geochimica et Cosmochimica Acta, Vol. 61, pp. 3671–3689.

Balashov, V., and Yardley, B. (1998). Modeling metamorphic fluid flow with reaction-compaction permeability

Feedbacks. American Journal of Science, Vol. 298, pp. 441–470.

Banks, P., Vargas, R., Rodríguez, G.I., Shagam, R. (1985). Zircon U-Pb ages from orthogneiss, Pamplona, Colombia. VI Cong. Latinoam. Geol. Bogotá. Resúmenes.

Barth, T. (1962). Theoretical Petrology. New York, J. Wiley & Sons.

Bence, A., and Albee, A. (1968). Empirical correction factors for the electron microanalysis of silicate and oxides. Journal of Geology, Vol. 76, pp. 382-403.

Bickle, M., and Baker, J. (1990). Advective-diffusive transport of isotopic fronts: An example from Naxos, Greece. Earth and Planetary Science Letters, Vol. 97, pp. 78–93.

Boinet, T., Bourgois, J., Bellon, H., and Toussaint, J. (1985). Age et repartition du magmatism premesozoique des Andes de Colombie. Comptes rendus hebdomadaires des séaces de L'Académie des Sciences. Serie D: Sciences Naturalles, Vol. 300(II), 445-450.

Brady, J. (1977). Metasomatic zones in metamorphic rocks. Geochimica et Cosmochimica Acta, Vol. 41, pp. 113-125.

Breeding, C., Ague, J., Brocker, M., and Bolton, E. (2003). Blueschist preservation in a retrograded, high-pressure, low-temperature metamorphic terrene, Tinos, Greece: Implications for fluid flow paths in subduction zones. Geochemistry, Geophysics, Geosystems, Vol. 4, 9002, doi:10.1029/2002GC000380.

Campos, N. (1999). Estudio Mineralógico y Petrográfico de las Metamorfitas al Occidente del Municipio de Mutiscua (Norte de Santander). Tesis de Pregrado, Universidad Industrial de Santander, Bucaramanga (Colombia).

Carlson, W. (2002). Scales of disequilibrium and rates of equilibration during metamorphism. American Mineralogist, Vol. 87, pp. 185-204.

Cardona, A. (2003). Correlacoes entre fragmentos do embasamento Pre-Mesozoico da terminacao setentrional dos Andes Colombianos, com base em datos isotopicos e geocronologicos. Dissertacao de Mestrado, Universidade de Sao Paulo, Instituto de Geociencias, 149pp.

Castellanos, O. (2001). Chemical composition of the rock-forming minerals in the Silgará formation and P-T conditions in the Mutiscua area, Santander Massif, Eastern Cordillera, Colombia. Unpublished Master Thesis, Shimane University, Matsue (Japan), 146pp.

Castellanos, O., Rios, C., and Takasu, A. (2004). Chemically sector-zoned garnets in the metapelitic rocks of the Silgará Formation in the central Santander Massif, Colombian Andes: occurrence and growth history. Boletín de Geología UIS, Vol. 26, pp 91-18.

Connolly, J.A.D. (1990). Multivariable phase diagrams: an algorithm based on generalized ther-

modynamics. American Journal of Science, Vol. 290, pp. 666-718.

Cui, X., Nabelek, P.I., and Mian, L. (2001). Heat and fluid flow in contact metamorphic aureoles with layered and transient permeability, with implication to the Notch Peak aureole, Utah. Journal of Geophysical Research, Vol. 106, pp. 6477-6491.

Cui, X., Nbelek, P.I., and Liu, M. (2003). Reactive flow of mixed CO_2-H_2O fluid and progress of calc-silicate reactions in contact metamorphic aureoles: insights from two-dimensional numerical modeling. Journal of Metamorphic Geology, Vol. 21, pp. 663–684.

Dörr, W., Grösser, J., Rodriguez, G., Kramm, U., 1995. Zircon U-Pb age of the Páramo Rico tonalite-granodiorite, Santander Massif (Cordillera Oriental, Colombia) and its geotectonic significance. Journal of South American Earth Sciences 8(2), 187-194.

Essene, E. (1983). Solid Solutions and Solvi among metamorphic carbonates with applications to geologic thermobarometry. In: Reviews in Mineralogy: Carbonates: Mineralogy and Chemistry. ed. Reeder, Richard J., Vol. 11. Book Crafters, Inc.: Chelsea, Michigan, pp. 77-96.

Essene, E. and Fyfe, W. (1967). Omphacite in Californian metamorphic rocks, Contributions to Mineralogy and Petrology, Vol. 15, pp. 1–23

Ferry, J. (1994). Overview of the petrologic record of fluid flow during regional metamorphism in northern New England. American Journal of Science, Vol. 294, pp. 905–988.

French, B.M. (1966). Some geological implications of equilibrium between graphite and a C-H-O gas phase at high temperatures and pressures. Reviews of Geophysics, Vol. 4, pp. 223-253.

Fritts, C. (1965). Bedrock geologic map of the Ansonia quadrangle, Fairfield and New Haven Counties, Connecticut. U.S. Geological Survey Quadrangle Map GQ-426.

García, C. y Castellanos O. (1998). Petrografía de la Formación Silgará en la Cordillera Oriental, Colombia. X Congreso Latinoamericano de Geología, Buenos Aires, Argentina, Memorias, T.2, 263-268.

García, C. and Ríos, C. (1998). Mineralogy and petrography of the metamorphic rocks to the west of Pamplona (Norte de Santander). Conference, XVI International Post-graduate Course in Metallogeny. June 9-21, 1997, Quito, Ecuador.

García, C., y Ríos, C. (1999). Metamorfismo y metalogenia asociada del Macizo de Santander, Cordillera Oriental, Colombia. Informe final Proyecto de Investigación. Universidad Industrial de Santander - Colciencias, p.191.

García, C., y Campos, N. (2000). Composición química y mineralogía de las biotitas metamórficas del sector central del Macizo de Santander, Colombia. Boletín de Geología UIS, Vol. 22 (37), 18-27.

García, C., Ríos, C., and Castellanos, O. (2005). Medium-pressure metamorphism of the Silgará Formation in the central Santander Massif, Eastern Cordillera, Colombian Andes: constraints for a collision model. Boletín de Geología UIS, Vol. 27 (2), 43-68.

Gélvez, J. and Márquez, R. (2002). Caracterización textural del granate y de sus elementos de deformación asociados, y modelamiento de su historia de nucleación y crecimiento en las rocas metapelíticas de la Formación Silgará en la región suroccidental del Macizo de Santander. Tesis de Pregrado, Universidad Industrial de Santander, Bucaramanga (Colombia).

Goldsmith, J., and Heard, C. (1961). Subsolidus phase relations in the system $CaC0_3$-$MgC0_3$. Journal of Geology, Vol. 69, pp. 45-74.

Goldsmith, J., and Newton, R. (1969). P-T-X relations in the system $CaC0_3$-$MgC0_3$ at high temperatures and pressures. American Journal of Science, Vol. 267-A, pp. 160-190.

Goldsmith, R., Marvin, R., and Mehnert, H. (1971). Radiometric ages in the Santander Massif, eastern

Cordillera, Colombian Andes. U.S. Geological Survey Professional Paper, Vol. 750-D, D41-D49.

Gómez, S.I. y Avila, G.A. (2006). Petrogénesis de las rocas calcosilicatadas que ocurren como bandas de reacción entre mármoles y rocas metapelíticas de la Formación Silgará, región Central del Macizo de Santander. Tesis de Pregrado, Universidad Industrial de Santander, Bucaramanga (Colombia).

Gordon, T., and Greenwood, H. (1971). The stability of grossularite in H_2O-CO_2 mixtures. American Mineralogist, Vol. 56, pp. 1674-1688.

Graf, D., and Goldsmith, J. (1955). Dolomite-magnesian calcite relations at elevated temperatures and CO_2 pressures. American Mineralogist, Vol. 51, pp. 353-80.

Greenwood, H. (1967). Wollastonite: stability in H_2O-CO_2 mixtures and occurrence in a contact-metamorphic aureole near Salmo, British Columbia, Canada. American Mineralogist, Vol. 52, pp. 1669-1680.

Harker. R., and Tuttle, O. (1955). Studies in the system CaO-MgO-CO_2. Part 2. Limits of solid solution along the binary join Ca CO3-MgCO3. American Journal of Science, Vol. 253, pp .274-282.

Hewitt, D.A. (1973). The metamorphism of micaceous limestones from south-central Connecticut. American Journal of Science, Vol. 273-A, pp. 444-469.

Hey M.H. (1954). A new review of the chlorites. Mineralogical Magazine, Vol. 30, pp. 277-292.

Powell, R., and Holland, T. (1988). An internally consistent dataset with uncertainties and correlations; 3, Applications to geobarometry, worked examples and a computer program. Journal of Metamorphic Geology, Vol. 6, pp. 173-204.

Hover-Granath, V., Papike, J., and Labotka, T. (1983). The Notch Peak contact metamorphic aureole: Petrology of the Big Horse limestone member of the Orr Formation. Geological Society of America Bulletin, Vol. 94, pp. 889-906.

Hunt, J., and Kerrick, D. (1977). The stability of sphene; experimental redetermination and geologic implications. Geochimica and Cosmochimica Acta, Vol. 41, pp. 279-288.

Joesten, R. (1977). Evolution of mineral assemblage zoning in diffusion metasomatism. Geochimica and Cosmochimica Acta, Vol. 41, pp. 649-670.

Joesten, R. (1991). Local equilibrium in metasomatic processes revisited: diffusion-controlled growth of chert nodule reaction rims in dolomite. American Mineralogist, Vol. 76, pp. 743-755.

Kerrick, D.M. (1977). The genesis of zoned skarns in the Sierra Nevada, California. Journal of Petrology, Vol. 18, pp. 144-181.

Kretz, R. (1980). Occurrence, Mineral Chemistry, and Metamorphism of Precambrian Carbonate Rocks in a Portion of the Grenville Province. Joumal of Petrology. Vol. 21(3), pp. 73-620.

Kretz, R. (1983). Symbols for rock-forming minerals. American Mineralogist, Vol. 68, pp. 277-279.

Leake, B. (1978). Nomenclature of amphiboles. Canadian Mineralogist, Vol. 16, pp. 501-520.

Leger, A., and Ferry, J. (1993). Fluid infiltration and regional metamorphism of the Waits River Formation, northeast Vermont, USA. Journal of Metamorphic Geology, Vol. 11, pp. 3–29.

López, V., and Soto, J. (1999). Metamorphism of calc-silicate rocks from the Alboran Basement. Zahn, R., Comas, M., and Klaus, A. (Eds.). Proceedings of the Ocean Drilling Program, Scientific Results, Vol. 161, pp. 251-259.

Mantilla, L., Ordoñez, J., Cepeda, S., and Ríos, C. (2001). Study of the paleofluids in the Silgará Formation and their relationship with deformation processes, Aratoca-Pescadero area (southwestern Santander Massif). Boletín de Geología UIS, Vol. 23(38), pp. 69-75.Mantilla, L., Ríos, C., and Castellanos, O. (2002). Study of the rehydratation process of the Silgará Formation metamorphic rocks, from the compositional

analysis of chlorite, southwestern Santander Massif. Boletín de Geología UIS, Vol. 24(39), pp. 7-17.

Mantilla, L., Ríos, C., Gélvez, J., Márquez, R., Ordoñez, J., and Cepeda, S. (2003). New evidences on the presence of a shear band in the metapelitic sequence of the Silgará Formation, Aratoca-Pescadero area (southwestern Santan- der Massif). Boletín de Geología UIS, Vol. 25(40), pp. 81-89

Meinert, L. (1992). Skarns and skarn deposits. Geoscience Canada, Vol. 19, pp. 145-162.

Moecher, D., and Essene, E. (1990). Phase equilibria for calcic scapolite, and implications of variable Al-Si disorder for P-T, T-X (sub CO_2), and alpha-X relations. Journal of Petrology, Vol. 31, pp. 997-1024.

Montenegro, G., y Barragán, M. (1999). Metamorfismo y evolución metamórfica del área comprendida entre los municipios de Vetas (Santander) y Mutiscua (Norte de Santander). Tesis de Pregrado, Universidad Industrial de Santander, Bucaramanga (Colombia).

Mora, C., and Valley, J. (1989). Halogen-rich scapolite and biotite; implications for metamorphic fluid-rock interaction. American Mineralogist, Vol. 74, pp. 721-737.

Nabelek, P. (2002). Calc-silicate reactions and bedding-controlled isotopic exchange in the Notch Peak aureole, Utah: implications for differential fluid fluxes with metamorphic grade. Journal of Metamorphic Geology, Vol. 20, pp. 429-440.

Oliver, N., Wall, V., and Cartwright, I. (1992). Internal control of fluid compositions in amphibolite-facies scapolitic calc-silicates, Mary Kathleen, Australia. Contributions to Mineralogy and Petrology, Vol. 111, pp. 94-112.

Ordoñez, J. (2003). Petrology and geochemistry of the granitoids at the Santander Massif, Eastern Cordillera, Colombian Andes. Unpublished Master Tesis, Shimane University, Matsue (Japan), 150pp.

Ordóñez, J., and Mantilla, L. (2004). Significance of an early Cretaceous Rb-Sr age in the Pescadero Pluton, Santander Massif. Boletín de Geología UIS, Vol. 26 (43), pp. 115-126.

Ordoñez-Carmona, O., Restrepo, J.J., and Martins, M. (2006). Geochronological and isotopical review of pre-Devonian crustal basement of the Colombian Andes. Journal of South American Earth Sciences, Vol .21(4), pp. 372-382.

Palin, J. (1992). Stable isotope studies of regional metamorphism in the Wepawaug Schist, Connecticut. PhD thesis, Yale University, New Haven, 170 p.

Piazolo, S. and Markl, G. (1999). Humite- and scapolite-bearing assemblages in marbles and calcsilicates of Dronning Maud Land, Antarctica: new data for Gondwana reconstructions. Journal of Metamorphic Geology, Vol. 17, pp. 91–107.

Ramberg, H. (1952). The Origin of metamorphic and metasomatic rocks. University of Chicago Press, Chicago.

Rice, J. (1977). Contact metamorphism of impure dolomitic limestone in the Boulder Aureole, Montana. Contributions to Mineralogy and Petrology, Vol. 59, pp. 237-259.

Restrepo-Pace, P. (1995). Late Precambrian to Early Mesozoic tectonic evolution of the Colombian Andes, based on new geochronological, geochemical and isotopic data. Unpublished PhD Thesis, University of Arizona, 195p.

Restrepo-Pace, P., Ruiz, J., Gehrels, G., and Cosca, M. (1997). Geochronology and Nd isotopic data of Grenville-age rocks in the Colombian Andes: New constraints for late Proterozoic-early Paleozoic Paleocontinental reconstruction of the Americas. Earth and Planetary Sciences Letters, Vol. 150, pp. 427-441.

Rice, J.M. (1977). Contact metamorphism of impure dolomitic limestone in the Boulder aureole, Montana. Contributions to Mineralogy and Petrology, Vol. 59, pp. 237-259.

Ríos, C. (2001). Occurrence, chemical composition and genetic significance of the biotite in the Silgará Formation metamorphic rocks, southwestern Santander Massif, Eastern Cordillera, Colombian Andes. Boletín de Geología UIS, Vol. 23(38), pp. 41-49.

Ríos, C. and García, C. (2001a). First occurrence of the three Al_2SiO_5 polymorphs in the Silgará Formation metapelitic rocks, southwestern Santander Massif, Eastern Cordillera, Colombian Andes. Boletín de Geología UIS, Vol. 23(38), pp. 51-59.

Ríos, C. and García, C. (2001b). Conditions of pressure and temperature of metamorphism in the Santander Massif, Eastern Cordillera, Colombian Andes. Conference, VIII Colombian Congress of Geology, Agosto 8-10 de 2001, Manizales, Colombia.

Ríos, C., García, C., and Takasu, A. (2003a). Tectono-metamorphic evolution of the Silgará Formation metamorphic rocks in the southwestern Santander Massif, Colombian Andes. Journal of South American Earth Sciences, Vol. 16, pp. 133-154.

Ríos, C., Gélvez, J., and Marquez, R. (2003b). Kynetics of the nucleation and growth garnet in the Silgará Formation metapelitic rocks, southwestern Santander Massif. Boletín de Geología UIS, Vol. 25(40), pp. 23-38.

Ríos, C. (2005). Cation substitutions governing the chemistry of amphibole in the Silgará Formation metabasites at the southwestern Santander Massif. Boletín de Geología UIS, Vol. 27(2), pp. 13-30.

Robinson, P. (1991). Eye of the petrographer, mind of the petrologist. American Mineralogist, Vol. 76, pp.1781-1810.

Rosen, O., Fettes, O, and Desmons, J. (2005). Chemical and mineral compositions of metacarbonate rocks under regional metamorphism conditions and guidelines on rock classification. Russian Geology and Geophysics, Vol. 46(4), pp. 351-360.

Rye, R.O., Schuiling, R.D., Rye, D.M., and Jansen, J.B.H. (1976). Carbon, hydrogen, and oxygen isotope studies of the regional metamorphic complex at Naxos, Greece. Geochimica et Cosmochimica Acta, Vol. 40, pp. 1031–1049.

Schäfer, J., Grösser, J., and Rodríguez, G., (1998). Proterozoic Formación Silgará, Cordillera Oriental, Colombia: metamorphism and geochemistry of amphibolites. Zbl. Geol. Paläont. Teil I, 1997 (3-6), Stuttgart, pp. 531-546.

Shmulovich, K., Graham, C., and Yardley, B. (2001). Quartz, albite, and diopside solubilities in H_2O-NaCl and H_2O-CO_2 fluids at 0.5-0.9 GPa. Contributions to Mineralogy and Petrology, Vol. 141, pp. 95–108.

Skippen, G. (1971). Experimental data for reactions in siliceous marble. Journal of Geology, Vol. 79, pp. 457-481.

Spear, F. (1993). Metamorphic Phase Equilibria and Pressure-Temperature-Time Paths. Mineralogical Society of America, Washington, DC, 799p.

Storre, B., and Nitsch, K.H. (1972). Die Reaction 2 Zoisit+CO_2 = Anorthit+Calcit+H_2O. Contributions to Mineralogy and Petrology, Vol. 35, pp. 1-10.

Tanner, P., and Miller, R. (1980). Geochemical evidence for loss of Na and K from Moinian calc-silicate pods during prograde metamorphism Geological Magazine, Vol. 117, pp. 267–275.

Thompson, A. (1971). P_{CO2} in low grade metamorphism; Zeolite, carbonate, clay mineral, prehnite relations in the system CaO-Al_2O_3-SiO_2-CO_2-H_2O. Contributions to Mineralogy and Petrology, Vol. 33, pp. 145-161.

Thompson, A. (1975). Calc-silicate diffusion zones between marble and pelitic schist. Journal of Petrology, Vol. 16, pp. 314-346.

Thompson, J., Jr. (1959). Local equilibrium in metasomatic processes. Researches in Geochemistry, Vol. 1, pp. 427-457.

Thompson, J., Jr. (1955). The thermodynamic basis for the mineral facies concept. American Journal of Science, Vol. 253, pp. 65-103.

Tracy, R., Rye, D., Hewitt, D., and Schiffries, C. (1983). Petrologic and stable-isotopic studies of fluid-rock interactions, south-central Connecticut: I. The role of infiltration in producing reaction assemblages in impure marbles. American Journal of Science, Vol. 283-A, pp. 589–616.

Vidale, R. (1969). Metasomatism in a chemical gradient and the formation of calc-silicate bands. American Journal of Science, Vol. 267, pp. 857–874.

Vidale, R., and Hewitt, D. (1973). "Mobile" components in the formation of calc-silicate bands. American Mineralogist, Vol. 58, pp. 991–997.

Walther, J. (1996). Fluid production and isograd reactions at contacts of carbonate-rich and carbonate poor layers during progressive metamorphism. Journal of Metamorphic Geology, Vol. 14, pp. 351–360.

Ward, D., Goldsmith, R., Cruz, B., Jaramillo, C., and Restrepo, H. (1973). Geología de los Cuadrángulos H-12, Bucaramanga y H-13, Pamplona, Departamento de Santander. U.S. Geological Survey e Ingeominas. Boletín Geológico, Vol. XXI(1-3), pp. 1-132.

Ward, D., Goldsmith, R., Cruz, B., Jaramillo, C., and Vargas, L. (1970). Mapa Geológico del Cuadrángulo H-13, Pamplona, Colombia. Ingeominas.

Widmer, T., and Thompson, A. (2001). Local origin of high pressure vein material in eclogite facies rocks of the Zermatt-Saas zone, Switzerland. American Journal of Science, Vol. 301, pp. 627–656.

Zarayskiy, G., Zharikov, V., Stoyanovskaya, F., and Balashov, V. (1987). The experimental study of bimetasomatic skarn formation. International Geology Review, Vol. 29, pp. 761-858.